이학박사 학위논문

The Role of Transglutaminase 2 in RANKL-Induced Osteoclast Differentiation

RANKL 에 의해 유도되는 파골세포 분화과정에서
Transglutaminase 2 의 역할

2014 년 8 월

서울대학교 대학원
치의과학과 세포및발생생물학 전공
김 우 신

RANKL 에 의해 유도되는 파골세포 분화과정에서 Transglutaminase 2 의 역할

지도교수 김 홍 희

이 논문을 이학박사학위논문으로 제출함

2014 년 4 월

서울대학교 대학원

치의과학과 세포및발생생물학 전공

김 우 신

김우신의 박사학위논문으로 인준함

2014 년 6 월

위 원 장 정 진 화 (인)

부위원장 김 홍 희 (인)

위 원 류 현 모 (인)

위 원 이 승 복 (인)

위 원 이 수 영 (인)

The Role of Transglutaminase 2 in RANKL-Induced Osteoclast Differentiation

by

Woo-Shin Kim

Advisor:

Prof. Hong-Hee Kim, Ph.D

A thesis submitted fulfillment of the requirements for the degree of Doctor of Philosophy in Seoul National University

June, 2014

Doctoral Committee:

Professor 허 지 나 , Chairman

Professor 김 홍 희 , Vice Chairman

Professor 류 현 모

Professor 이 승 복

Professor 이 수 영

ABSTRACT

The Role of Transglutaminase 2 in RANKL-Induced Osteoclast Differentiation

Woo-Shin Kim

Department of Cell and Developmental Biology

The Graduate School

Seoul National University

(Directed by Prof. Hong-Hee Kim, Ph.D)

Transglutaminase 2 (TG2) is a multifunctional protein that can perform functions as transglutaminase, protein kinase, cell surface adhesion mediator, G protein, protein disulfide isomerase and isopeptidase depending on stimuli. Several studies have shown the effect of transglutaminase 2 on bone formation. TG2 has been reported to be required for fibronectin and type I collagen matrix deposition. However, functions of TG2 in bone metabolism still remain unclear and TG2 has not yet been examined in osteoclastogenesis.

Therefore, this study was carried out to clarify whether TG2 regulates osteoclastogenesis. First, I found that TG2, among TG family members, was

selectively expressed in osteoclast precursors and pre-fusion osteoclasts (pOCs). I next used TG2 siRNA and TG2 knockout mice to investigate the role of TG2 in osteoclast differentiation. I confirmed that reduction of TG2 increased formation of tartrate-resistant acid phosphatase (TRAP)-positive multinucleated cells (MNCs). Western blot and real-time PCR analyses demonstrated that the TG2 deficiency significantly increased the expression of osteoclastogenic transcription factors such as c-fos and nuclear factor of activated T cell c1 (NFATc1). Moreover, reduction of TG2 augmented the activation of MAPKs, ERK, JNK and p38, and NF-κB signaling pathways by RANKL. In addition, I found that the TG2 deficiency increased nuclear translocation of NFATc1 and p65. Consequently, TG2 deficiency resulted in a potent increase of sealing zone formation and bone resorption activity. In contrast, TG2 overexpression suppressed osteoclast formation and expression of osteoclastogenic genes in RAW264.7 cells. B lymphocyte induced maturation protein 1 (Blimp1) has been shown to be a positive regulator of osteoclastogenesis and to be induced by the activation of NF-κB signaling pathway. As TG2 was reported to suppress Blimp1 expression, I investigated the interrelationship between TG2 and Blimp1 in osteoclast differentiation. I found that reduction of TG2 increased Blimp1 expression in BMMs and pOCs. Furthermore, the augmentation of osteoclastogenesis by TG2 knockdown was attenuated by Blimp1 knockdown.

In addition, TG2 knockout mice exhibited lower bone mass compared to wildtype mice. Bone histomorphometry revealed higher number and surface area of osteoclasts in TG2 knockout mice. In conclusion, these results indicate that TG2 plays an inhibitory role in osteoclast differentiation and function via Blimp1.

Keywords : Osteoclast differentiation, Transglutaminase 2, c-fos, NFATc1, NF-κB, Blimp1

Student Number: 2009-31131

CONTENTS

LIST OF FIGURES

LIST OF TABLES

ABBREVIATIONS

TG2	Transglutaminase 2
M-CSF	Macrophage-colony stimulating factor
RANK	Receptor activator of nuclear factor κB (NF-κB)
RANKL	Receptor activator of nuclear factor κB (NF-κB) ligand
BMMs	Bone marrow derived-macrophages
pOCs	Pre-fusion osteoclasts
NFATc1	Nuclear factor of activated T cell c1
TRAP	Tartrate-resistant acid phosphatase
MNCs	Multinucleated cells
Blimp1	B lymphocyte induced maturation protein 1
MAPKs	Mitogen-activated protein kinases
ERK	Extracellular signal-regulated kinase
JNK	c-Jun N-terminal kinase
AP-1	Activator protein-1
ATP6v0d2	v-ATPase subunit d2
DC-STAMP	Dendritic cell-specific transmembrane protein
SZ	Sealing zone
BV/TV	Bone volume per tissue volume

Tb.Th	Trabecular thickness
Tb.N	Trabecular number
Tb.sp	Trabecular separation
N.Oc/B.Pm	Number of osteoclasts per bone perimeter
Oc.S/BS	Osteoclast surface per bone surface
ES/BS	Eroded surface per bone surface
N.Ob/B.Pm	Number of osteoblasts per bone perimeter
RT-PCR	Reverse transcriptase polymerase chain reaction
siRNA	Small interfering ribonucleic acid

I. Introduction

Bone is a dynamic tissue that is continuously remodeled and maintained by a coupled action of osteoclasts and osteoblasts (Martin and Sims, 2005; Mukherjee and Rotwein, 2012). Osteoclasts and osteoblasts regulate the bone homeostasis by balancing the activities of bone resorption and bone formation, respectively (Fig. 1). Thus, the imbalance in bone remodeling can lead to bone diseases such as osteoporosis, periodontal disease, Paget's disease, and rheumatoid arthritis (Braun and Zwerina, 2011; Harada and Rodan, 2003; Teitelbaum, 2000; Walsh et al., 2006).

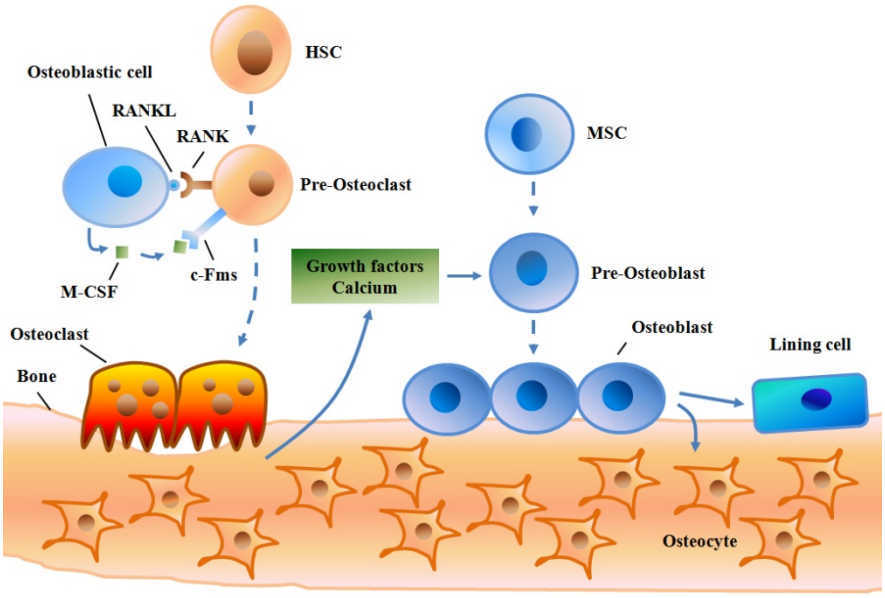

Modified from Nature Reviews Cancer Vol. 11 June 2011

Figure 1. Osteoclast-osteoblast coupling.

Osteoblastic cell produces osteoclast differentiation factor RANKL and M-CSF. Haematopoietic stem cells (HSCs) undergo differentiation to osteoclasts by RANKL stimulation. HSC-derived osteoclasts resorb bone and release growth factors and calcium. Osteogenic factors, growth factors and calcium induce osteoblast differentiation from mesenchymal stem cells (MSCs). Osteoblasts replace the resorbed bone with new bone. Some osteoblasts become osteocytes and lining cells.

1. Osteoclast differentiation

Osteoclasts are tartrate-resistant acid phosphatase (TRAP)-positive multinucleated cells (MNCs) that differentiate from the monocytes/macrophages of hematopoietic lineage cells (Hayashi et al., 1998; Teitelbaum et al., 1997). Osteoclast differentiation is induced by stimulation of two major factors, macrophage-colony stimulating factor (M-CSF) and receptor activator of nuclear factor κB (NF-κB) ligand (RANKL) (Fig. 2). M-CSF is critical for monocyte/macrophage lineage commitment (Valledor et al., 1998). M-CSF binds to its receptor, c-Fms, on osteoclast precursor cells and induces the expression of receptor activator of NF-κB (RANK), which is the receptor on these cells for RANKL (Arai et al., 1999). RANKL initiates its signal transduction through binding to RANK and induces the differentiation and fusion of osteoclast precursor cells into mature osteoclasts (Boyle et al., 2003; Suda et al., 1999). In particular, RANKL stimulates the activation of NF-κB and mitogen-activated protein kinases (MAPKs), including extracellular signal-regulated kinase (ERK), c-Jun N-terminal kinase (JNK) and p38 (Asagiri and Takayanagi, 2007; Iotsova et al., 1997; Wong et al., 1998). RANKL stimulation also induces c-fos expression and thus activates the activator protein-1 (AP-1)

complex containing c-fos and c-jun (Wagner and Eferl, 2005). RANKL-induced activation of NF-κB and AP-1 complex is required for the induction of nuclear factor of activated T-cells cytoplasmic 1 (NFATc1), a key transcription factor for osteoclast differentiation (Grigoriadis et al., 1994; Khosla, 2001). NFATc1 is auto-amplified by binding to NFAT binding sites on its own promoter (Asagiri et al., 2005; Nakashima and Takayanagi, 2011). In addition to its essential role in early differentiation, NFATc1 is likely to be involved in regulating osteoclast function. TRAP is responsible for bone resorption activity (Takayanagi et al., 2002). v-ATPase subunit d2 (ATP6v0d2) (Lee et al., 2006) and dendritic cell-specific transmembrane protein (DC-STAMP) (Kukita et al., 2004; Yagi et al., 2005) were shown to be essential for mononuclear osteoclast fusion. These genes are directly induced by NFATc1 during osteoclastogenesis (Kim et al., 2008; Reddy et al., 1995). Mature osteoclasts form a ring-shaped sealing zone (SZ) for contact with the bone surface (Kanehisa et al., 1990; Saltel et al., 2004; Tehrani et al., 2006). These active osteoclasts resorb the bone matrix by secreting acid and proteases, such as TRAP, cathepsin K and matrix metalloprotease 9 (MMP9) within the resorption pit (lacuna) for bone degradation (Georgess et al., 2014).

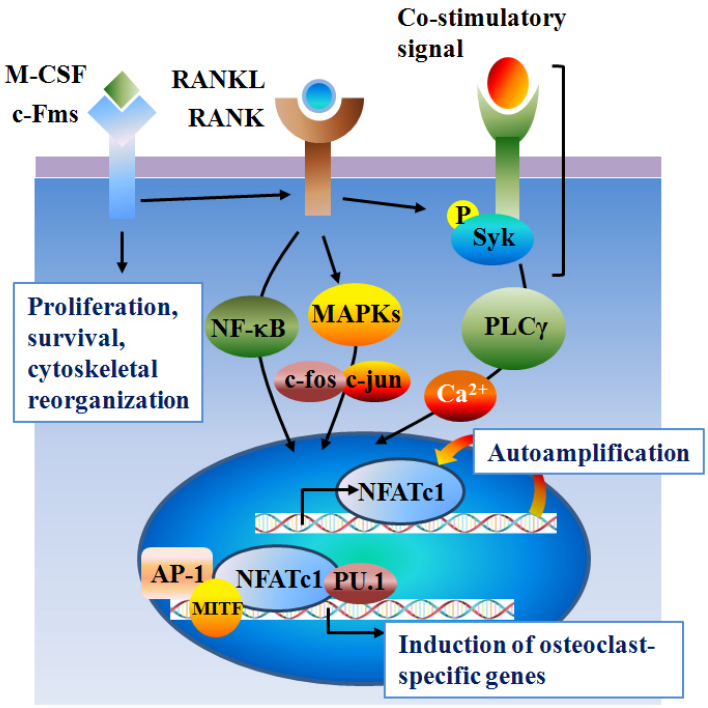

Modified from Trends in Endocrinology and Metabolism Vol. 23 November 2012

Figure 2. Schematic representation of osteoclast differentiation.

M-CSF and RANKL are key cytokines during osteoclast differentiation. M-CSF regulates proliferation, survival and cytoskeletal reorganization and induces RANK expression. RANKL binds to its specific membrane-bound receptor RANK and activates NF-κB, MAPKs, calcium signaling pathways which are crucial for the induction of NFATc1. NFATc1 is autoamplified by binding to an NFAT-binding site on its own promoter. NFATc1, together with AP-1, MITF and PU.1, induces various osteoclast-specific genes.

2. Role of Blimp1 in osteoclast differentiation

B lymphocyte induced maturation protein 1 (Blimp1) (encoded by *Prdm1*) is a zinc finger transcriptional repressor and plays crucial roles in the differentiation and/or function of various kinds of cells such as macrophages and lymphocytes (Martins and Calame, 2008). In particular, Blimp1 has been shown to function as a master regulator of terminal differentiation of antibody-secreting B lymphocytes through direct repression of transcription factors (Shapiro-Shelef et al., 2003) and homeostasis of effector T cells (Calame et al., 2003; Martins et al., 2006), and specification of primordial germ cells (Ohinata et al., 2005; Vincent et al., 2005). Blimp1 was originally identified as a silencer of *IFN-β* gene transcription (Keller and Maniatis, 1991) and has been reported to be regulated by various transcription factors, such as NF-κB (Johnson et al., 2005; Morgan et al., 2009; Sen, 2006; Wang et al., 2009), AP-1 (Vasanwala et al., 2002; Yu et al., 2012), STAT3 (Kwon et al., 2009; Reljic et al., 2000) and IRF-4 (Gupta et al., 2001; Sciammas et al., 2006). Blimp1 was also reported to be important for osteoclast differentiation and to be induced early by NFATc1 upon RANKL stimulation (Zhao and Ivashkiv, 2011) (Fig. 3). Blimp1 suppresses expression of anti-osteoclastogenic genes such as interferon

regulatory factor-8 (IRF-8) and v-maf musculoaponeurotic fibrosarcoma oncogene family, protein B (MafB), which were observed to be repressed during osteoclastogenesis (Nishikawa et al., 2010; Smink et al., 2009). Moreover, IRF-8 and MafB was reported to negatively regulate expression and function of NFATc1 during osteoclastogenesis (Kim et al., 2007; Wagner, 2010; Zhao et al., 2009). Eventually, this repression of IRF-8 and MafB by Blimp1 seems to ensure maintenance of NFATc1 activity during osteoclastogenesis.

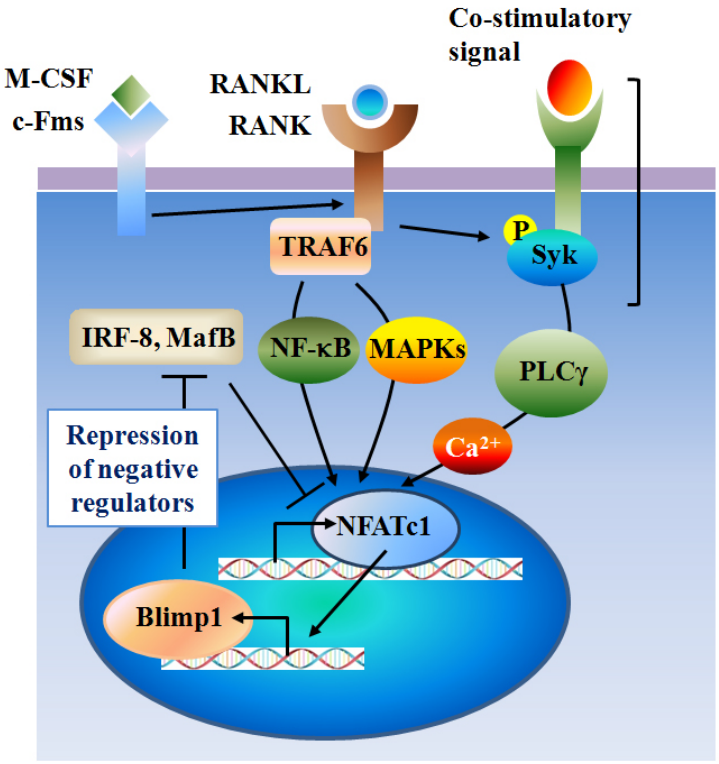

Modified from Trends in Endocrinology and Metabolism Vol. 23 November 2012

Figure 3. The mechanism of Blimp1 in osteoclast differentiation.

RANKL stimulation recruits TRAF6 and activates NF-κB, MAPKs and co-stimulatory signaling pathways. Activation of these signaling pathways up-regulates NFATc1 expression. Subsequently NFATc1 induces Blimp1 expression which suppresses negative regulators, IRF-8, MafB and Bcl6. Next, NFATc1 is auto-amplified and induces osteoclast specific genes.

3. Function of transglutaminase family

Transglutaminase (TG) family consists of at least 8 distinct members (Table 1): factor XIII A (Griffin et al., 2002), TG1 (or keratinocyte TG), TG2 (or tissue TG), TG3 (or epidermal TG), TG4 (or prostate TG), TG5 (or TG X), TG6 (or TG Y), and TG7 (or TG Z). Transglutaminase family catalyzes three types of Ca^{2+}-dependent posttranslational modification reactions: transamidation, esterification, and hydrolysis. These reactions play important roles in various biological processes such as proliferation (Barone et al., 2007; Dardik et al., 2007), differentiation (Balajthy et al., 2006; Steinert et al., 1996; Sturniolo et al., 2003), cell death (Datta et al., 2007; Fesus and Szondy, 2005; Sarang et al., 2005; Yuan et al., 2005), inflammation (Kim et al., 2002; Quan et al., 2005), cell migration (Akimov and Belkin, 2001; Kang et al., 2004), and wound healing (Inada et al., 2000; Nahrendorf et al., 2006). TG2 acts as a multifunctional protein due to multiple functional domains and the functions of TG2 depend on the cellular localization and its regulators (Fig. 4). In addition to Ca^{2+}-dependent catalytic activity, TG2 is distinguished from other family members by several unique characteristics such as ubiquitous expression, non-enzymatic functions of GTPase activity, and cell-matrix interaction (Zemskov

et al., 2006). Ca^{2+} and GTP are two important regulators, which act as switches between the two distinct functions, transglutaminase (Iismaa et al., 2009; Lorand and Graham, 2003; Steinert et al., 1999) and GTPase (Begg et al., 2006a; Begg et al., 2006b; Di Venere et al., 2000; Iismaa et al., 2000) activities, via an allosteric modulation of TG2 conformation.

Table 1.

Characterization of transglutaminase

Identified forms of TG	Synonyms	Residues (molecular mass in kDa)	Gene	Prevalent function
Factor XIII A	Catalytic A subunit of Factor XIII found associated with B subunit in plasma as A2B2 heterotetramer. Fibrin stabilizing factor	732 (83)	F13A1	Blood clotting and wound healing
TG1	Keratinocyte Tgase	814 (90)	TGM1	Cell envelope formation in the differentiation of keratinocytes
TG2	Tissue Tgase	686 (80)	TGM2	Cell death and cell differentiation, matrix stabilization, adhesion protein
TG3	Epidermal Tgase	692 (77)	TGM3	Cell envelope formation during terminal differentiation of keratinocytes
TG4	Prostate Tgase	683 (77)	TGM4	Reproductive function involving semen coagulation particularly in rodents
TG5	Tgase X	719 (81)	TGM5	Epidermal differentiation
TG6	Tgase Y		TGM6	Not characterized
TG7	Tgase Z	710 (80)	TGM7	Not characterized

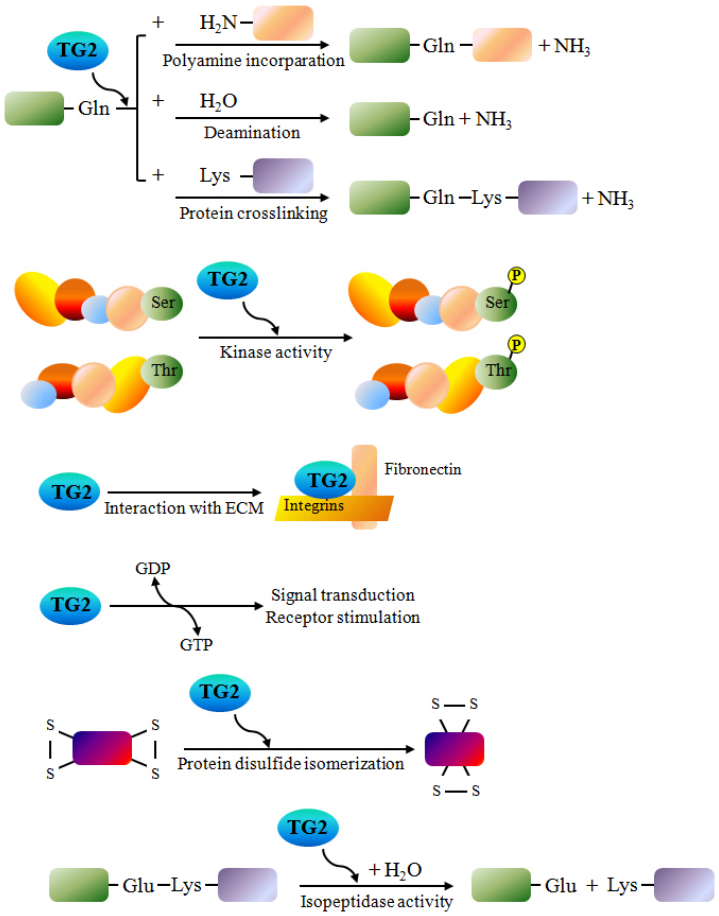

Modified from FEBS Journal Vol. 278 October 2011

Figure 4. Biochemical activities of transglutaminase 2

TG2 is a multifunctional protein containing multiple subcellular compartments. TG2 has functions as transglutaminase, protein kinase, cell surface adhesion mediator, G protein, protein disulfide isomerase and isopeptidase. Functions of TG2 regulate differentiation, cell death, inflammation, cell migration and wound healing in various cells.

4. Purpose of this study

Several studies have reported effects of transglutaminase family members, especially TG2 and factor XIII A, on bone formation and metabolism (Nurminskaya and Kaartinen, 2006). TG2 and factor XIII A regulate the matrix crosslinking and extracellular matrix assembly which act as the major regulator of mineralization (Al-Jallad et al., 2011; Al-Jallad et al., 2006). In addition to regulating matrix mineralization and osteoblast differentiation, TG2 is expressed in hypertrophic condrocytes, and chondrocyte-derived transglutaminase induced the differentiation of primary osteoblasts leading to increased matrix calcification (Heath et al., 2001; Nurminskaya et al., 2003). Despite these studies, the relationship of TG2 with osteoclastogenesis has yet to be elucidated. To gain better knowledge in the crucial role of TG2 *in vitro* and *in vivo*, I examined whether TG2 is involved in regulation of osteoclastogenesis through loss- and gain-of-function approaches.

II. Materials and methods

1. Animals

TG2 knockout mice generated by Vincenzo De Laurenzi (De Laurenzi and Melino, 2001) were provided by Prof. In-Gyu Kim (Seoul National University, College of Medicine, Korea). All mice were fed a regular diet and water and maintained on a 12 hr light/night cycle at the animal facility of Seoul National University School of Dentistry. 5-wk-old ICR mice for isolation of primary bone marrow derived-macrophages (BMMs) were purchased from OrientBio, Korea. All animal experiments were performed with the approval of the Institutional Animal Care and Use Committee at Seoul National University.

2. Reagents

Recombinant RANKL and M-CSF were from Peprotech EC Ltd. (London, UK). Anti-TG2, anti-c-fos, anti-NFATc1, anti-α-tubulin and NF-κB inhibitor BAY 11-7085 were purchased from Santa Cruz Biotechnology (Santa Cruz, CA, USA). Anti-Blimp1 was purchased from Abcam (Cambridge, UK). Polyclonal antibodies against ERK, JNK, p38, IκB, phospho-ERK, phospho-JNK, phospho-p38, phospho-IκB and PARP were purchased from Cell Signaling

Technology (Cambridge, MA, USA). Monoclonal antibody against β-actin and horseradish peroxidase (HRP)-conjugated secondary antibodies were from Sigma Aldrich (St Louis, MO, USA). NFATc1 and NF-κB p65 Transcription Factor Assay Kits were purchased from Active Motif (Carlsbad, CA, USA). Cell counting kit-8 (CCK) was obtained from Dojindo (Kumamoto, Japan). NE-PER Nuclear and Cytoplasmic extraction reagents kit was obtained from Pierce Biotechnology (Rockford, lL, USA). BrdU cell proliferation assay kit was purchased from Calbiochem (Darmstadt, Germany). TRAP staining kit and other reagents were purchased from Sigma Aldrich.

3. Bone marrow derived-macrophages (BMMs) generation

Bone marrow of tibiae and femurs of 5-wk-old mice were flushed with α-MEM (Welgene, Daegu, Korea). After removing erythrocytes with hypotonic buffer, cells were cultured in α-MEM containing 10% FBS for 24 hr and adherent cells were discarded. Non-adherent bone marrow cells were transferred onto 100 mm non-coated Petri dishes at 5×10^6 cells per dish and cultured in the presence of M-CSF (30 ng/ml) for 3 days. Adherent cells at this stage were considered bone marrow derived-macrophages (BMMs) after the non-adherent cells were washed out.

4. Cell culture

BMMs were cultured in α-MEM supplemented with 10% (v/v) heat-inactivated FBS, 100 units/ml of penicillin and 100 μg/ml of streptomycin, and incubated at 37°C in 5% CO_2. BMMs were plated in 60 mm dish at 5×10^5 cells and 48-well culture plates at 4×10^4 cells per well. RAW264.7 and 293FT cells were cultured in DMEM supplemented with 10% (v/v) heat-inactivated FBS, 100 units/ml of penicillin and 100 μg/ml of streptomycin, and incubated at 37°C in 5% CO_2. RAW264.7 cells were plated in 48-well culture plates at 1×10^4 cells per well and 293FT cells were plated in 60 mm culture dishes at 4×10^5 cells.

5. Preparation of cytoplasmic and nuclear protein lysates

Cytoplasmic and nuclear protein lysate were prepared from BMMs using the NE-PER Nuclear and Cytoplasmic extraction reagents kit (Pierce Biotechnology) according to the manufacturer's instructions. In brief, cultured cells were washed with PBS and treated with cell lysis buffer. After centrifugation, the cleared supernatant was transferred to a new tube as cytoplasmic extract. The nuclear pellet was washed twice and lysed with nuclear lysis reagent. After centrifugation, the cleared supernatant was used as

the nuclear protein extract. Protein concentration was determined using a detergent-compatible colorimetric assay kit (Bio-Rad Laboratories, CA, USA).

6. RT-PCR and quantitative real-time PCR

Total RNA was extracted from BMMs and RAW264.7 cells at the indicated time points. After isolation of total RNA using TRIZOL (Invitrogen), reverse transcription was performed using 2 μg of total RNA and a superscript II reverse transcriptase (Invitrogen) according to the manufacturer's protocol. For amplification of TG family, RT-PCR was performed with a cycle of denaturation at 95°C for 15 sec and annealing/extension at 60°C for 60 sec for 26 cycles. PCR products were separated in a 1.5% agarose gel and stained with ethidium bromide. Expression of target genes was analyzed using the *HPRT* housekeeping gene as an input control. Real-time PCR was performed with the ABI 7500 real-time system using KAPA SYBR FAST qPCR kit (Kapa Biosystems, MA, USA). The detector was programmed with the following PCR conditions: 40 cycles for 3 sec denaturation at 95°C and 33 sec amplification at 60°C. All reactions were run in triplicates and were normalized using the *HPRT* gene, and values indicating the fold-change from control are shown. Relative differences in PCR results were evaluated by the comparative cycle threshold method. All primer sets for RT-PCR and real-time PCR are listed in Table 2.

7. Gene cloning and lentivirus gene transduction

To generate TG2 overexpressed stable RAW264.7 cells, the 2061 bp cDNA (GenBank accession number NM_009373.3) fragment of *TGM2* was obtained by RT-PCR of mRNA from BMMs. The PCR reaction steps included initial denaturation at 95°C for 5 min followed by reaction cycles of denaturation at 95°C for 30 sec, annealing at 56°C for 30 sec, and extension at 72°C for 4 min. The following primers were used: *TG2*, 5′-GGACTAGTGCCACCATGGCAGAGGAGCTGCTC -3′ (sense) and 5′-TCCCCGCGGGGCCGGGCCGATGATAAC-3′ (antisense). pLenti6 lentiviral vector and PCR product were cleaved with SpeI and SacII restriction enzymes and subjected to 1% agarose gel electrophoresis. Each DNA fragment was purified from the gel and *TG2* fragment was cloned into identical sites of pLenti6 vector. To generate lentiviral particles, 293FT cells were transfected with pLenti6-LacZ (control) or pLenti6-TG2 plasmid using polyfect transfection reagent. Viral supernatant was harvested after 48 hr and passed through 0.45 μm syringe filter. RAW264.7 cells were infected with viral supernatant mixed with polybrene (6 μg/ml) for 18 hr. After overnight incubation, infected RAW264.7 cells were selected with blasticidin (1:2000) for 15 days. Forced expressions of each construct were determined by amounts of mRNA and protein expression levels.

8. Cell proliferation assay

TG2 knockdown (BrdU assay) and knockout (CCK assay) BMMs were cultured for 1-3 days. After TG2 knockdown, BMMs were subjected to BrdU assay following the manufacturer's instruction. For CCK assay, TG2 knockout BMMs were incubated with 10% CCK solution in cell culture medium for 30 min at 37°C. After incubation, optical density was measured with an ELISA reader at 450 nm.

9. Western blot

BMMs and RAW264.7 cells were lysed with a lysis buffer containing 120 mM Tris–HCl (pH 7.5), 150 mM NaCl, 1 mM EDTA, 1 mM EGTA, 0.5% NP40, 2.5 mM sodium pyrophosphate, 1 mM β-glycerophosphate, 1 mM Na_3VO_4, 1 mM NaF, and protease inhibitors (Roche, Mannheim, Germany). The protein concentration of cell lysates was determined by Dc protein assay kit (Bio-Rad, Hercules, CA, USA) and equal amounts of protein were loaded onto 10 or 12% SDS-polyacrylamide gel. After transfer onto nitrocellulose membranes (Amersham Pharmacia, Uppsala, Sweden) and blocking with 5% nonfat skim milk, primary antibodies were added and incubated for overnight at 4°C. The immunoreactivity was detected with ECL reagents (Pierce, Rockford,

IL, USA) after incubation with HRP-conjugated secondary antibodies for 1 hr in 2% skim milk. Comparable loading was verified by reprobing the same membranes with anti-β-actin antibody.

10. TRAP staining and osteoclast measurement

To generate osteoclasts, BMMs and RAW 264.7 cells were plated in 48-well tissue culture plates at density of 4×10^4 cells/well and 1×10^4 cells/well, respectively. Cells were cultured in the presence or absence of RANKL (100 ng/ml) for 3 or 4 days. The BMMs culture was supplemented with M-CSF (30 ng/ml). The culture medium was changed at day 2. Under this condition, TRAP-positive mononuclear cells were detected at day 2 and TRAP-positive multinucleated cells (MNCs) were observed at days 3 and 4. The cells were fixed with 3.7% formaldehyde for 30 min at room temperature. After permeabilized with 0.1% Triton X-100 for 5 min, TRAP staining was performed in the dark for 30 min using a TRAP kit following the manufacturer's instructions. After staining, cells were washed with distilled water and observed under a light microscope. On light microscopy, osteoclasts were seen as TRAP-positive multinucleated ($\geq$ 3 nuclei) cells. The total number of TRAP-positive MNCs and the surface area per TRAP-positive MNCs were measured using the Osteomeasure software (OsteoMetrics, Inc. Decatur, GA, USA). The

morphological features of osteoclasts were also photographed.

11. Resorption assay

BMMs were seeded on dentine discs (Osteosite Dentine Discs, Immunodiagnostic Systems Inc, Boldon, United Kingdom) and stimulated with RANKL for 7 days. There were typically 4 dentine discs per group. Cells were removed with 5% sodium hypochlorite for 10 min. Discs were wiped using cotton swab and rinsed with distilled water. Photographs were taken, and the area and depth of resorption pits were measured with a Carl Zeiss LSM 5-PASCAL laser-scanning microscope (Carl Zeiss Microimaging GmbH, Goettingen, Germany). Results are expressed as the resorbed area and depth per resorption pit.

12. Confocal microscopy

BMMs were seeded on glass cover slips in 24-well plates at a density of 7×10^4 cells per well. Cultured cells were fixed with 3.7% formaldehyde and permeabilized with 0.1% triton X-100. After blocking in PBS containing 1% BSA, cover slips were incubated with suitable primary antibodies (1:100) of each experiment for overnight at 4°C. Subsequently, cells were washed and

incubated with suitable Alexa Fluor® 647, FITC- or Cy3-conjugated secondary antibodies (1:250) of each experiment for 1 hr at room temperature. For sealing zone formation assay, BMMs were cultured in the presence of M-CSF (30 ng/mL) and RANKL (100 ng/ml) in α-MEM supplemented with 10% FBS. After 3 days in culture, mature osteoclasts were fixed and stained using rhodamine-phalloidin (red; actin) and DAPI (blue; nucleus). The mean intensity of sealing zone per osteoclast was measured using Zen 2009 software (Carl Zeiss). For p65 nuclear translocation assay, BMMs were serum-starved for 5 hr and stimulated with RANKL (500 ng/ml) for the indicated time. Stimulated cells were fixed and performed immunocytochemistry staining using anti-laminB (green; nucleus) and anti-p65 (red; p65). For NFATc1 nuclear translocation assay, BMMs were cultured in the presence of M-CSF (30 ng/mL) and RANKL (100 ng/ml). After 2 days in culture, osteoclast precursors were fixed and stained using anti-laminB (green; nucleus), anti-NFATc1 (red; NFATc1) and anti-TG2 (blue; TG2). The cover slips were mounted and cell images were obtained using a Zeiss LSM 700 confocal microscope (Carl Zeiss Microimaging GmbH, Goettingen, Germany).

13. Three-dimensional microcomputed tomography analysis

Femurs of 13-week old female TG2 knockout mice and WT littermate mice (6 per genotype) were fixed in 4% (vol/vol) paraformaldehyde for overnight and analyzed by micro-computed tomography (micro-CT) using the SkyScan 1072 system (SkyScan, Kontich, Belgium). Trabecular bone parameters were measured in the trabecular regions 1 mm away from 1 mm below the proximal edge of growth plate in the distal end of the femur. A total of 350-400 tomographic slices were acquired and three-dimensional analyses were performed with CT-volume software (ver 2.1.1.0; Skyscan).

14. Histomorphometrical analysis

Bone histomorphometric analyses were performed on paraffin-embedded sections. In brief, femurs were fixed in 4% paraformaldehyde, decalcified in 12% EDTA for 4 wk, and embedded in paraffin. The paraffin blocks were serially sectioned at a thickness of 6 μm and stained with TRAP/ hematoxylin or hematoxylin/eosin according to standard procedures. Trabecular bone parameters were analyzed using the Osteomeasure software and morphological features of tissue were also photographed.

15. Statistical analysis

All values represent mean ± SD. Statistical significance was determined using the Student t test (two-tailed distribution with two-sample equal variance) for *in vitro* and *in vivo* studies. For judgment, P values less than 0.05 was considered to be statistically significant.

Table 2.

Primers for RT-PCR and quantitative real-time PCR experiments

Gene		Sequence	Size (bp)	GenBank accession #
(TG family)		5'- -3'		
mouse *TG1*	Sense	CATTGGCACACTCATTGTCA	143	NM_001161715
	Antisense	ACACATTAGGTTTGCTGCCA		
mouse *TG2*	Sense	TATGATGCACCCTTCGTGTT	135	NM_009373
	Antisense	GCCCACACTCTTAGTGCTGA		
mouse *TG3*	Sense	CCATTGGCAAATACATCAGC	148	NM_009374
	Antisense	CCGAAAGATGCGTTAGGTTT		
mouse *TG4*	Sense	TTGTGTTCACGGAGGTCAAT	150	NM_177911
	Antisense	TATCTTCACGCCTGTTCTCG		
mouse *TG5*	Sense	GGTGTTCCTAAAGGCTCTGC	142	NM_028799
	Antisense	ATCACTGGGTTGAAGGGAAG		
mouse *TG6*	Sense	CAGGTGCATCAGTACCAAGG	138	NM_001289747
	Antisense	CAGGCTTCCACACTTAGCAG		
mouse *TG7*	Sense	CCAATTTCCATTCTGCACAC	136	NM_001160424
	Antisense	ATCATCCAGCACTCATTCCA		
mouse *Factor XIII A*	Sense	TGAGCTCCAAACTCACCAAG	145	NM_028784
	Antisense	CGGTACATGCCATCACTGTT		
(OC makers)		5'- -3'		
mouse *c-fos*	Sense	ACTTCTTGTTTCCGGC	233	NM_010234
	Antisense	AGCTTCAGGGTAGGTG		
mouse *NFATc1*	Sense	CCAGTATACCAGCTCTGCCA	188	BC061509
	Antisense	GTGGGAAGTCAGAAGTGGGT		
mouse *TRAP*	Sense	CGACCATTGTTAGCCACATACG	77	BC019160
	Antisense	TCGTCCTGAAGATACTGCAGGTT		
mouse *DC-STAMP*	Sense	GGGTGCTGTTTGCCGCTG	132	NM_029422
	Antisense	CGACTCCTTGGGTTCCTTGCT		
mouse *Atp6v0d2*	Sense	AGTGCAGTGTGAGACCTTGG	133	NM_175406
	Antisense	TCTGCAGAGCTTCTTCCTCA		
mouse *Blimp1*	Sense	GCCCAGTGTCACAAGAGCTA	141	NM_007548
	Antisense	GCTGATGTCGAACCTCTCAA		
(control)		5'- -3'		
mouse *HPRT*	Sense	GTGATTAGCGATGATGAACCA	149	NM_013556
	Antisense	CCCATCTCCTTCATGACATCT		

III. Results

1. TG2, among TG family members, is selectively expressed in BMMs and pOCs.

To investigate the expression pattern of TG family members in BMMs and osteoclast precursors, BMMs were cultured in the presence or absence of RANKL for 2 days. Among the TG family members, TG2 was dominantly expressed in both BMMs and pOCs treated with RANKL for 2 days. Factor XIII A was weakly detected. In contrast to TG2 and factor XIII A, other TG members were not detected (Fig. 5).

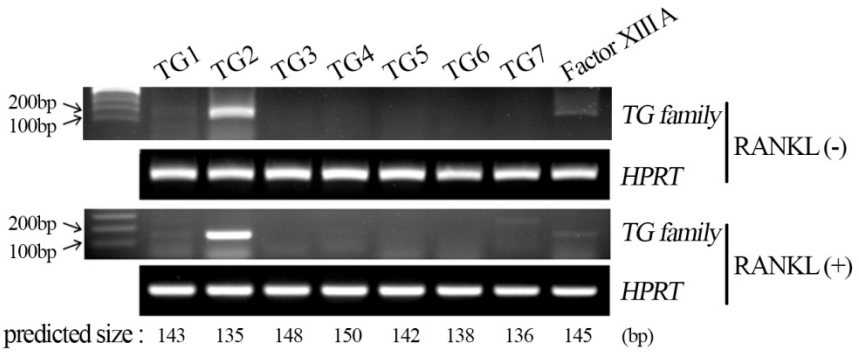

Figure 5. TG2 is selectively expressed in BMMs and pOCs.

BMMs were treated with M-CSF (30 ng/ml) with or without RANKL (100 ng/ml) for 2 days. mRNA expression for *TG1-TG7* and *factor XIII A* was analyzed by RT-PCR. The data shown are representative of three independent experiments.

2. TG2 knockdown increases osteoclast differentiation induced by RANKL.

Next, the effect of TG2 in the osteoclast differentiation was examined using the siRNA knockdown system. To do this, control or TG2 siRNA was transfected to BMMs. These cells were then treated with RANKL, and examined for knockdown efficiency. Quantitative real-time PCR analyses showed that TG2 mRNA levels were reduced more than 50% in the TG2 siRNA transfected BMMs and this extent of reduction was sustained (Fig. 6A). Western blotting experiments also showed suppression of TG2 by siRNA at the protein levels (Fig. 6B).

To confirm the effect of TG2 knockdown on osteoclast formation, I examined that BMMs were transfected with TG2 siRNA and incubated with RANKL for 3 days. When TG2 was knockdowned during osteoclastogenesis, the generation of TRAP-positive MNCs was enhanced (Fig. 7A). Moreover, the number of the TRAP-positive MNCs was also increased by TG2 knockdown (Fig. 7B). c-fos and NFATc1 are master transcriptional factors in RANKL-induced osteoclast differentiation. I therefore investigated whether TG2 knockdown affects the expression of c-fos and NFATc1. These results demonstrate that expression

levels of c-fos and NFATc1 were significantly increased in TG2 knockdowned cells (Fig. 7C, D). These data indicate that TG2 knockdown enhances RANKL-dependent osteoclast differentiation.

A

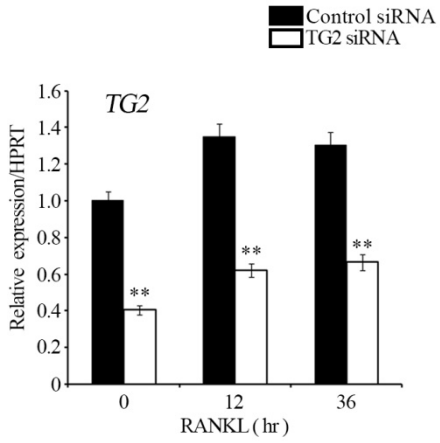

B

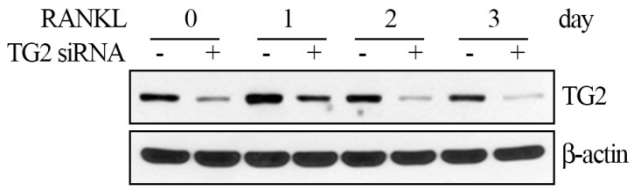

Figure 6. TG2 siRNA efficiently decreased TG2 mRNA and protein levels.

BMMs were transfected with control or TG2 siRNA for 18 hr and stimulated with RANKL for the indicated times. (A) mRNA level of *TG2* was measured using real-time PCR. Gene expression was normalized using the *HPRT* housekeeping gene, and values indicating the fold-change from control are shown. (B) Whole cell lysates were subjected Western blot analysis with anti-TG2. Real-time PCR data shown are representative of three independent experiments performed in triplicate. **, $p < 0.005$ versus stimulation with RANKL alone. All data are expressed as mean ± SD.

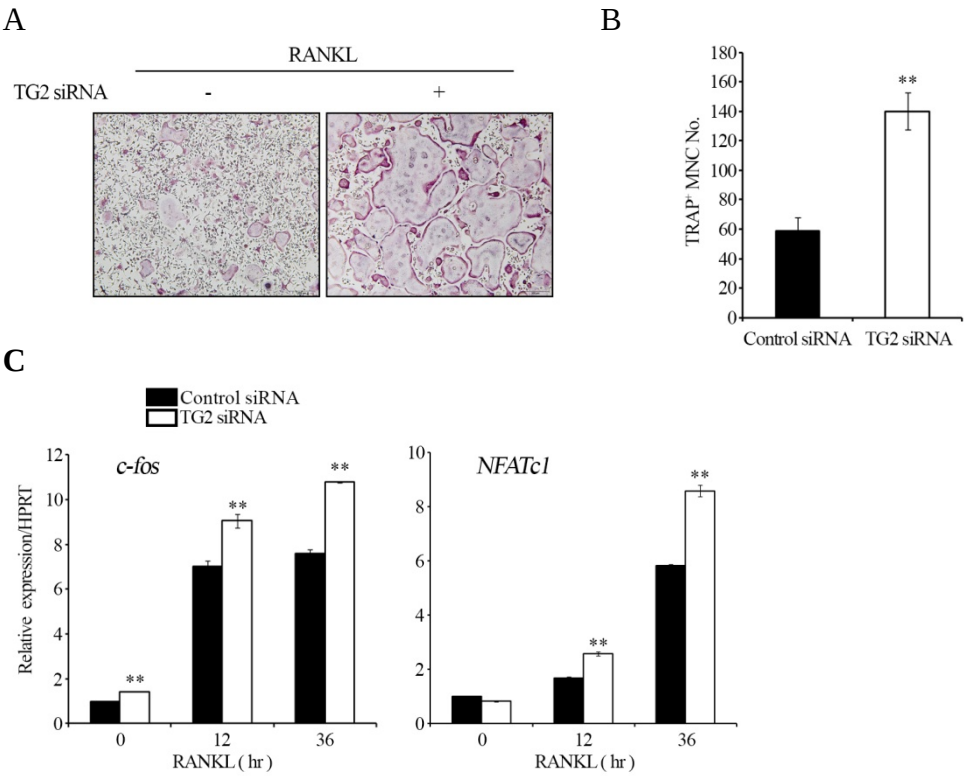
A
RANKL
TG2 siRNA
-
+
B
TRAP+ MNC No.
180
160
140
120
100
80
60
40
20
0
**
Control siRNA
TG2 siRNA
C
Control siRNA
TG2 siRNA
c-fos
NFATc1
Relative expression/HPRT
12
10
8
6
4
2
0
**
0
12
36
RANKL (hr)
D
RANKL
0
1
2
3
day
TG2 siRNA
- + - + - + - +
c-fos
NFATc1
β-actin

Figure 7. TG2 knockdown increased osteoclast formation by RANKL.

(A) TG2 knockdowned BMMs were stimulated with RANKL for 3 days, and TRAP staining was performed. (B) TRAP-positive MNCs (≥3 nuclei) were counted as osteoclasts. Scale bar, 200 μm. (C) mRNA levels of *c-fos* and *NFATc1* were measured using real-time PCR. (D) Whole cell lysates were subjected Western blot analysis with c-fos and NFATc1 antibodies. The data shown are representative of three independent experiments performed in triplicate. **, $p < 0.005$ versus stimulation with RANKL alone. All data are expressed as mean ± SD.

3. TG2 knockdown promotes bone resorption activity.

To explore further the influence of TG2 knockdown on osteoclast activity, the expression levels of genes encoding proteins related to osteoclast fusion and bone resorption activity were examined using real-time PCR. The expression of osteoclast activity related genes (*TRAP*, *DC-STAMP* and *ATP6v0d2*) was increased in TG2 knockdowned cells (Fig. 8). Next, the effect of TG2 knockdown on the resorption activity of osteoclasts was investigated. Consistent with the observations of the increase of c-fos and NFATc1, and the number of TRAP-positive MNCs, TG2 knockdown caused an increase in the resorbed area and depth per osteoclast (Fig. 9A, B).These data indicate that regulation of TG2 expression in osteoclasts affects a significant mechanism to control not only osteoclastogenesis but also osteoclast activity.

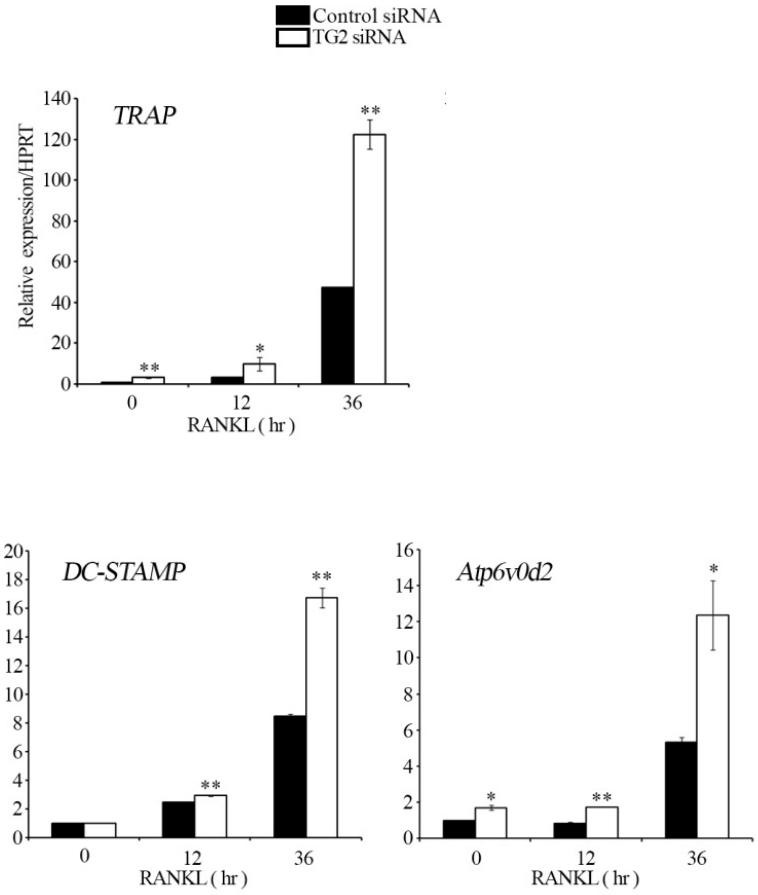

Figure 8. TG2 knockdown increased the expression of osteoclast activity related genes.

mRNA was isolated from the control siRNA or TG2 siRNA transfected BMMs at the indicated times. Expression of *TRAP, DC-STAMP* and *ATP6v0d2* were analyzed by real-time PCR. *, $p < 0.05$; **, $p < 0.005$ versus stimulation with RANKL alone. All data are expressed as mean ± SD.

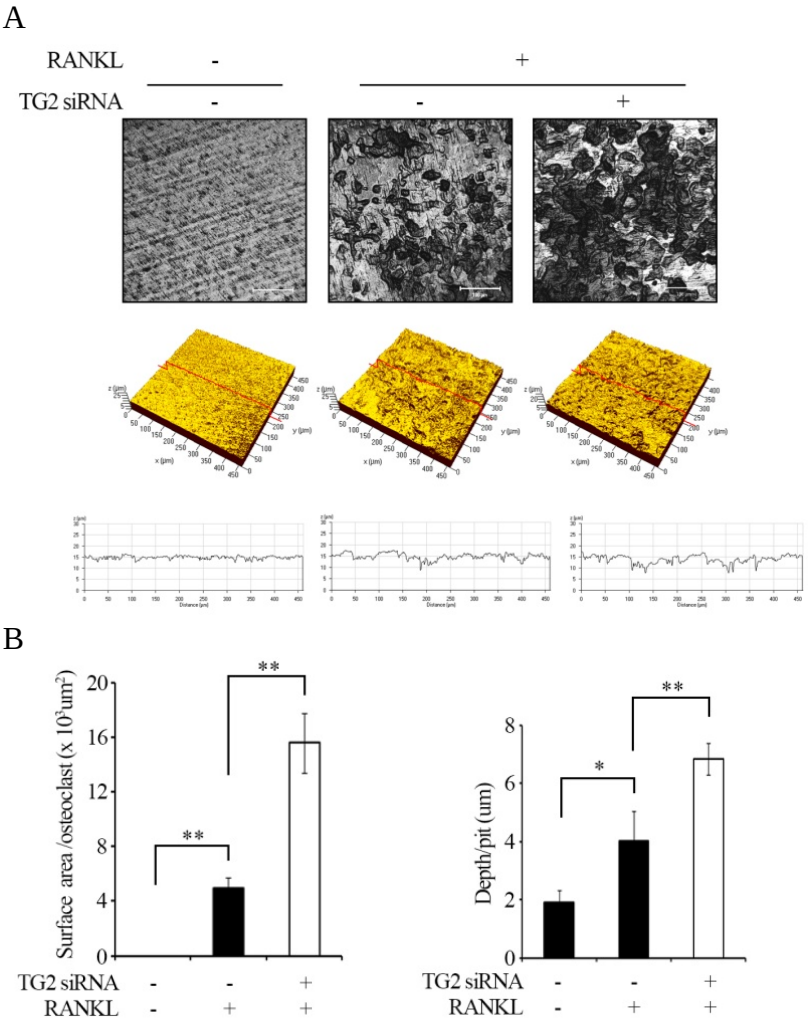

Figure 9. TG2 knockdown stimulated the osteoclast resorption activity.

(A) BMMs were transfected with control or TG2 siRNA and dentine resorption assay was performed. Black areas indicate resorbed lacunae on dentin slice. Scale bar, 100 μm. (B) Resorbed area and depth per osteoclast were calculated from randomly selected four images. *, $p < 0.05$; **, $p < 0.005$ versus stimulation with RANKL alone. All data are expressed as mean ± SD.

4. TG2 knockdown activates the RANKL-induced MAPKs and NF-κB signaling pathways.

To determine the intracellular mechanism of TG2 action, I investigated the activation of MAPKs involved in the RANKL signaling pathway. BMMs were stimulated with RANKL and the activation state of ERK, JNK and p38 activation was determined by Western blot analysis using phosphorylated form detectable antibodies. RANKL induced the activation of all three MAPKs at 5 and 15 min. In TG2 knockdown BMMs, the phosphorylation of ERK, JNK and p38 was greater than the control BMMs, whereas total levels of MAPKs were not changed (Fig. 10A). I next examined the effect of TG2 on the growth of BMMs (Fig. 10B). TG2 had little effect on the growth of BMMs, although TG2 knockdown slightly increased BrdU incorporation on day 1.

NF-κB signaling pathway is one of the crucial signaling pathways in RANKL-induced osteoclast differentiation. It has been well investigated that phosphorylation of IκB and transcriptional activity of p65 were enhanced by RANKL stimulation in osteoclast precursors (Iotsova et al., 1997; Wong et al., 1998). To investigate whether TG2 knockdown regulates NF-κB signaling pathway, we examined the phosphorylation level of IκB in osteoclast precursors.

RANKL stimulation induced phosphorylation of IκB within 5 min, and the level of RANKL-induced IκB phosphorylation was further enhanced by TG2 knockdown at 5 and 30 min (Fig. 11A). I further examined whether p65 transcriptional activity was increased in TG2 knockdown BMMs. The p65 transcriptional activity assay showed that the TG2 knockdown increased the activity of p65 at 15 min (Fig. 11B). These results suggest that TG2 knockdown increased the activation of the MAPKs and NF-κB signaling pathways by RANKL, without affecting the proliferation of ostoclast precursor cells.

A B

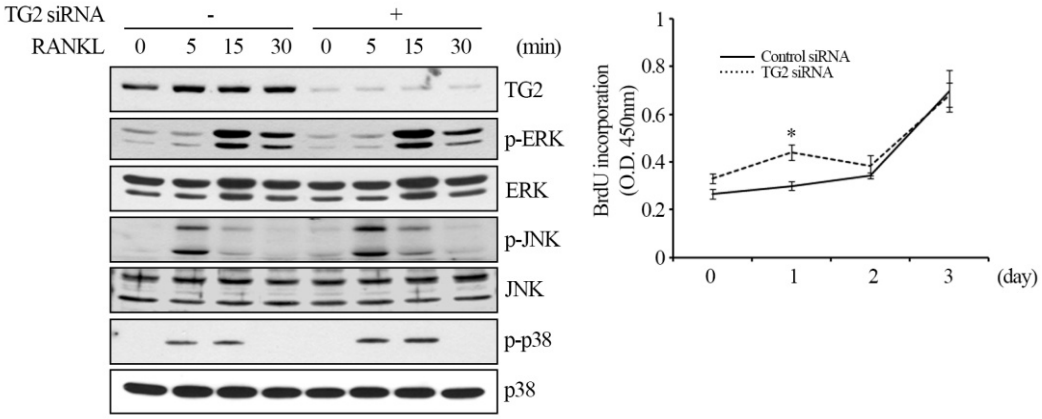

Figure 10. TG2 knockdown enhanced the activation of MAPKs signaling pathway by RANKL.

(A) At 48 hr after siRNA transfection, BMMs were serum starved for 5 hr and stimulated with RANKL (500 ng/ml) for the indicated times. Whole cell lysates were subjected to Western blot analysis with MAPKs pathway relevant antibodies. (B) BMMs were cultured for the indicated time and BrdU assay was performed. *, $p < 0.05$ versus stimulation with RANKL alone. All data are expressed as mean ± SD.

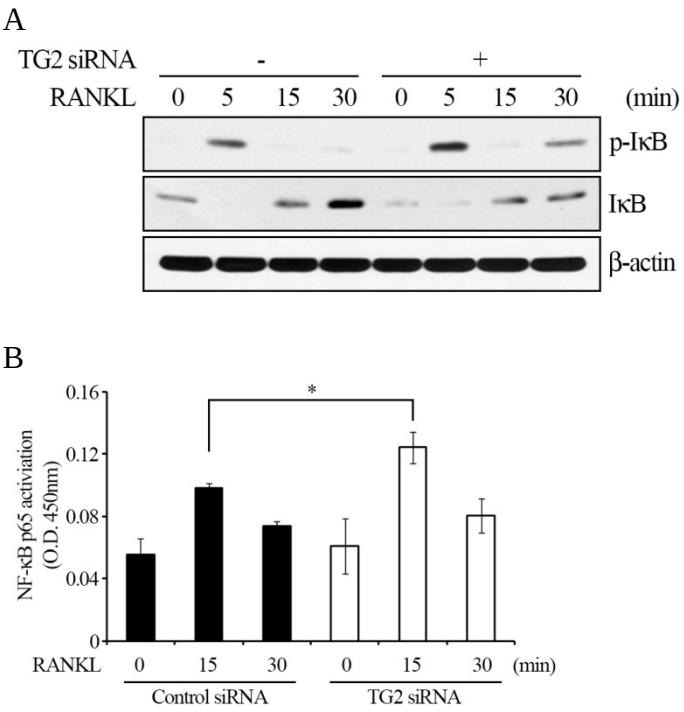

Figure 11. TG2 knockdown increased the activation of NF-κB signaling pathway by RANKL.

BMMs were transfected with control or TG2 siRNA. (A) At 48 hr after transfection, BMMs were serum starved for 5 hr and stimulated with RANKL (500 ng/ml) for the indicated times. Whole cell lysates were subjected to Western blot analysis with phospho-IκB and IκB antibodies. (B) Nuclear fraction was harvested from cultured cells and subjected to p65 Transcription Factor Assay. *, $p < 0.05$ versus stimulation with RANKL alone. All data are expressed as mean ± SD.

5. TG2 knockdown up-regulates Blimp1 expression by enhancing the NF-κB signaling pathway.

To explore the target of TG2, I examined the mRNA and protein expression levels of Blimp1 in TG2 knockdown cells for the indicated times. The mRNA expression level of Blimp1 by TG2 knockdown was much higher than that by control siRNA transfection (Fig. 12A). I also observed that TG2 knockdown enhanced the RANKL-induction of Blimp1 proteins in BMMs and pOCs (Fig. 12B). I further examined whether the increase of Blimp1 by TG2 knockdown was due to activation of NF-κB pathway. Inhibition of NF-κB pathway with BAY 11-7085 attenuated the induction of Blimp1 (Fig. 13A, B). BAY 11-7085 also significantly down-regulated the stimulation of RANKL-dependent induction of NFATc1 by TG2 knockdown (Fig. 13B). Interestingly, the expression level of c-fos was not affected by BAY 11-7085 treatment. These results suggest that TG2 regulates Blimp1 expression during RANKL-dependent osteoclast differentiation through NF-κB signaling pathway.

A

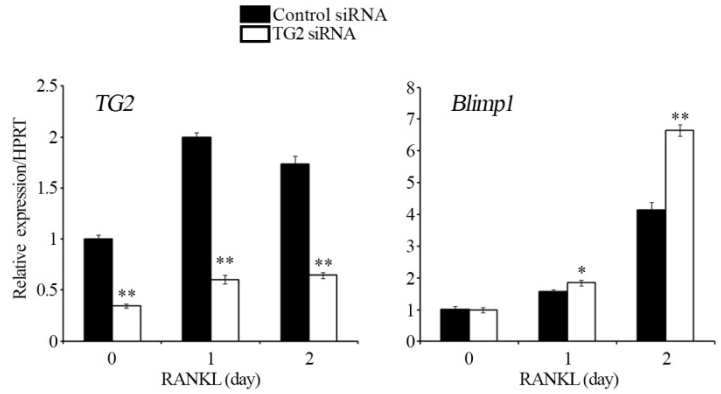

B

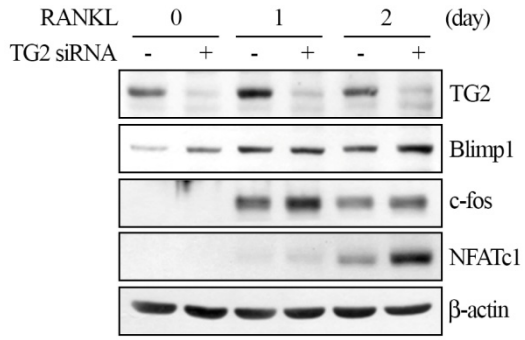

Figure 12. TG2 knockdown increased Blimp1 expression.

BMMs were transfected with control or TG2 siRNA. (A, B) siRNA transfected BMMs were cultured for the indicated times in the presence of M-CSF and RANKL. Expression of TG2 and Blimp1 was examined by real-time PCR (A) and Western blot (B) analyses. *, $p < 0.05$; **,$p < 0.005$ versus stimulation with RANKL alone. All data are expressed as mean ± SD.

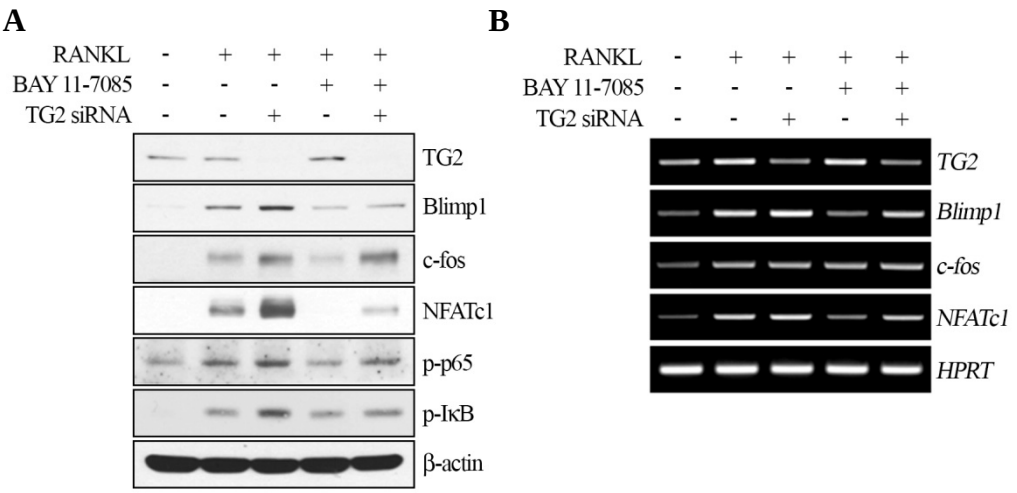

Figure 13. TG2 knockdown increased Blimp1 induction by RANKL through activation of NF-κB signaling pathway.

BMMs were transfected with control or TG2 siRNA. (A, B) TG2 siRNA transfected BMMs were cultured with or without BAY 11-7085 (5 μM) for 2 days. (A) Western blot analysis was performed to assess the expression of the indicated proteins. (B) PCR was performed to analyze the mRNA expression levels of *TG2, Blimp1*, *c-fos* and *NFATc1*. The data represent means of at least three independent experiments.

6. Blimp1 knockdown attenuates the up-regulation of NFATc1 by TG2 suppression.

To further clarify the role of the TG2/Blimp1 axis in RANKL-induced osteoclastogenesis, I investigated the alteration of osteoclast formation by TG2 and/or Blimp1 knockdown. As previously shown, TG2 knockdown significantly enhanced the formation of the TRAP-positive MNCs by RANKL. This enhancement of osteoclast formation by TG2 knockdown was significantly reduced by Blimp1 knockdown (Fig. 14A, B). Not only the number of TRAP-positive MNCs but also the size of TRAP-positive MNCs were decreased by knockdown of TG2 and Blimp1 (Fig. 14B, C).

I further examined whether knockdown of TG2 and Blimp1 affects the expression of c-fos and NFATc1. Osteoclast precursors transfected with TG2 and Blimp1 siRNA were stimulated by RANKL treatment for 2 days and subjected to Western blot and real-time PCR to determine expression levels of both protein and mRNA (Fig. 15A, B). Western blot and real-time PCR analyses revealed that TG2 knockdown increased expression level of NFATc1. Interestingly, a decrease of Blimp1 was associated with a significant reduction in the up-regulation of NFATc1 by TG2 knockdown. In contrast, expression

level of c-fos was only slightly affected by Blimp1 knockdown (Fig. 15A, B). These results indicate that Blimp1 knockdown was able to down-regulate protein and mRNA induction of NFATc1 by TG2 knockdown.

Next, I investigated the effects of TG2 knockdown on change in intranuclear level of NFATc1. Analyses of NFATc1 levels in cytoplasmic and nuclear fractions revealed an increase of expression and nuclear translocation of NFATc1 by TG2 knockdown. Moreover, TG2 knockdown increased total Blimp1 protein level compare with control cells in nuclear fractions (Fig. 16A). Similar results were obtained in NFATc1 transcription factor assay. Transcriptional activity of NFATc1 was increased by TG2 knockdown at day 2 after RANKL treatment (Fig. 16B). Thus, these data verify that TG2 knockdown up-regulates NFATc1 expression and transcriptional activity via Blimp1 induction during osteoclast differentiation.

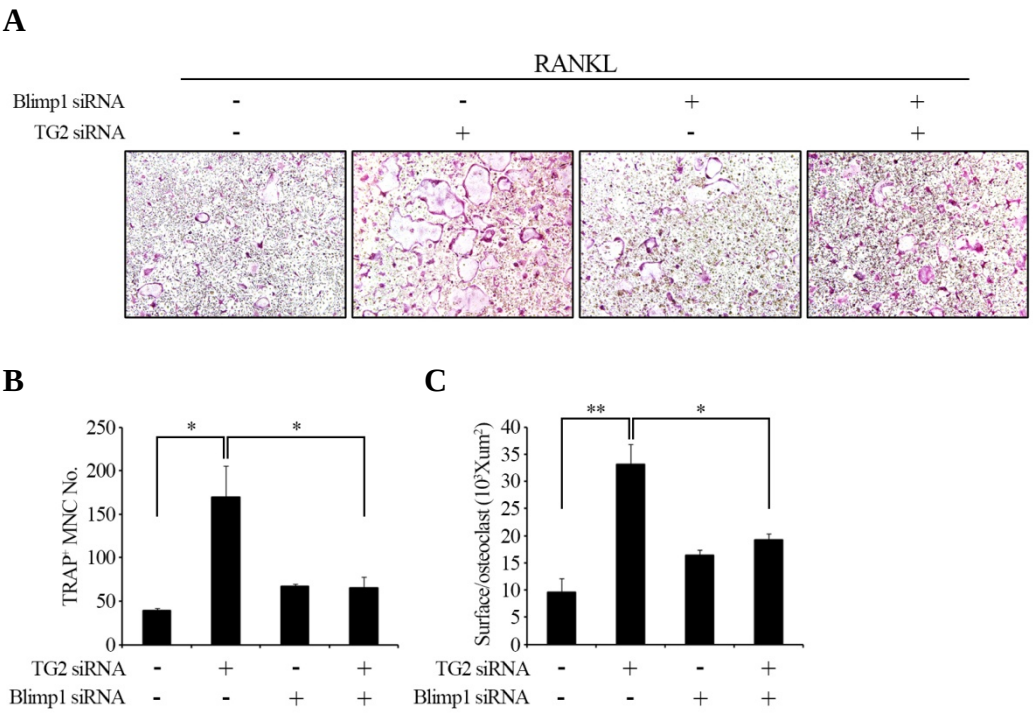

Figure 14. Blimp1 knockdown attenuated the induction of osteoclast formation by TG2 knockdown.

BMMs were transfected TG2 and/or Blimp1 siRNA. (A) TG2 and Blimp1 knockdowned BMMs were cultured for 3 days with M-CSF and RANKL. Cultured cells were fixed and stained for TRAP. (B) Number of TRAP-positive MNCs was counted and surface per osteoclast was measured. The data represent means of at least three independent experiments performed in triplicate. *, $p < 0.05$; **, $p < 0.005$. All data are expressed as mean ± SD.

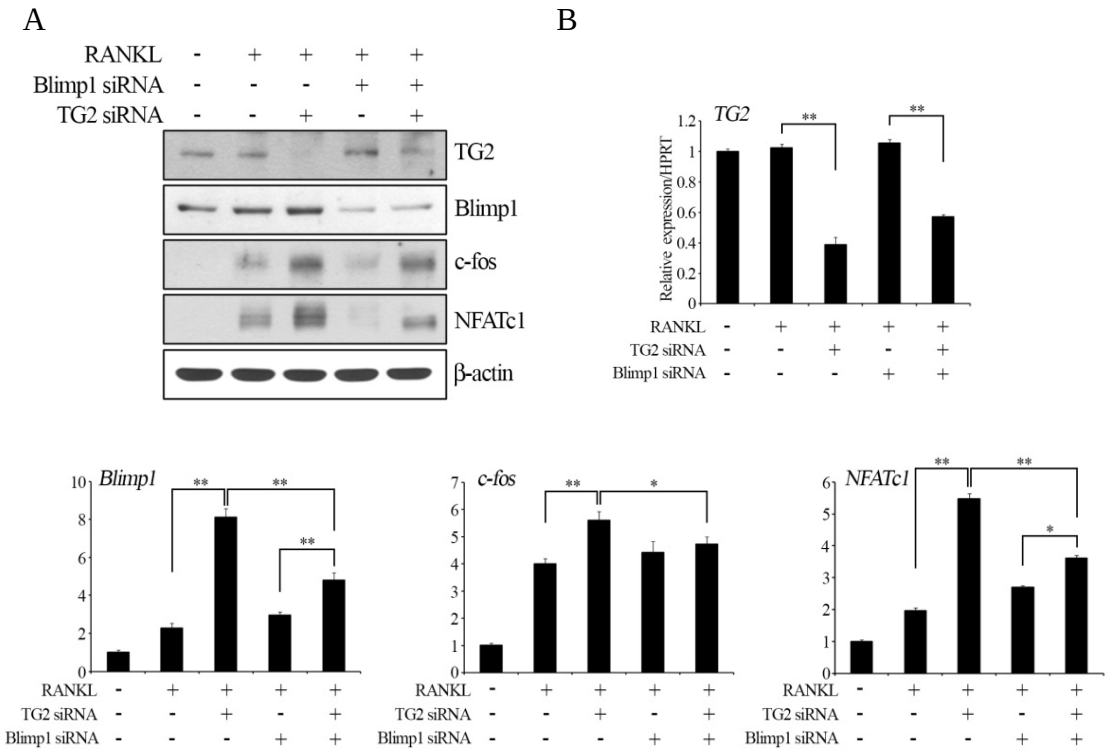

Figure 15. Blimp1 knockdown attenuated the up-regulation of NFATc1 by TG2 knockdown.

BMMs were transfected with TG2 and/or Blimp1 siRNA. (A, B) After TG2 and Blimp1 knockdown, BMMs were analyzed by Western blot (A) and real-time PCR (B) at day 2 after RANKL treatment. The data represent means of at least three independent experiments performed in triplicate. $p < 0.005$. All data are expressed as mean ± SD.

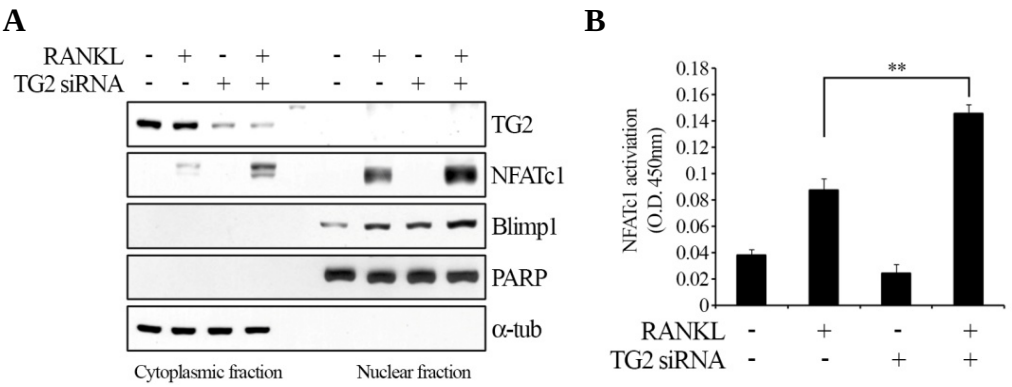

Figure 16. TG2 knockdown increased the nuclear translocation and transcriptional activity of NFATc1.

BMMs were transfected TG2 and/or Blimp1 siRNA. (A) Cytoplasmic and nuclear fractions were obtained from cells cultured for 2 days using fractionation kit and subjected to Western blot analysis for detection of NFATc1 and Blimp1. Antibodies for α-tubulin and PARP (full length) were used for the normalization of cytoplasmic and nuclear extracts, respectively. (B) NFATc1 transcriptional activity in nuclear extract was quantified by NFATc1 transcription factor assay. The data represent means of at least three independent experiments performed in triplicate. **, $p < 0.005$. All data are expressed as mean ± SD.

7. TG2 overexpression suppresses RANKL-induced osteoclast differentiation in RAW264.7 cells.

To confirm that TG2 has a negative role in osteoclast differentiation, I examined that TG2-overexpressing lentivirus was transduced into RAW264.7 cells and selected using the lentiviral-based system. I analyzed the expression level of TG2 in control and TG2-overexpressing stable RAW264.7 cells. Expression level of TG2 was significantly increased in TG2-overexpressing stable RAW264.7 cells (Fig. 17A, B). And I performed experiments using stable RAW264.7 cells as a gain-of-function approach. TG2 overexpression significantly suppressed RANKL-induced osteoclast formation (Fig. 17C). TG2 overexpression also reduced the number of TRAP-positive MNCs and the surface area per osteoclast (Fig. 17D). More importantly, Real-time PCR analysis showed that TG2 overexpression potently reduced mRNA levels of *c-fos*, *NFATc1* and *Blimp1* in differentiation condition (Fig. 18A). In addition, TG2 overexpression significantly decreased protein expression of c-fos, NFATc1 and Blimp1 (Fig. 18B). These results support the notion that TG2 plays a negative role in osteoclast differentiation.

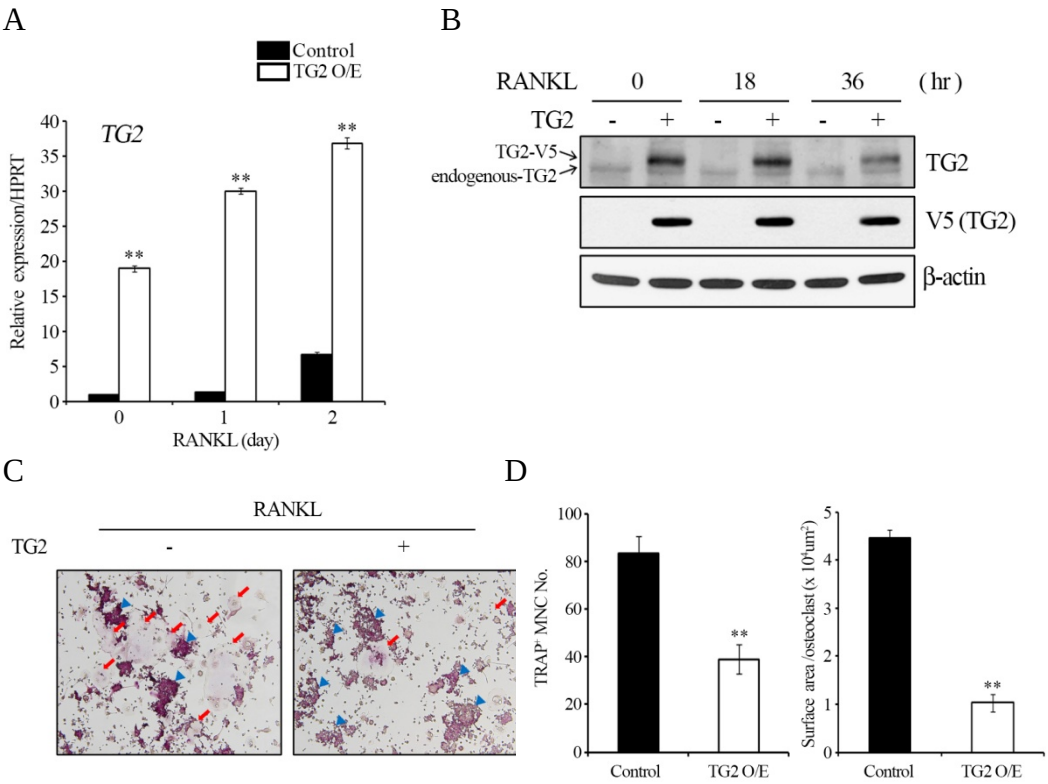

Figure 17. TG2 inhibited the expression of c-fos, NFATc1 and Blimp1 in RAW264.7 cells.

(A) *TG2* mRNA level was measured using real-time PCR. (B) Whole cell lysates were subjected to Western blot analysis with V5 antibody. Anti-V5 antibody was used to detect overexpressed TG2-V5. (C) TG2-overexpressing stable RAW264.7 cells were stimulated with RANKL for 4 days, and TRAP staining was performed. Red arrow: MNCs. Blue arrowhead: mononucleated cells. (D) TRAP-positive MNCs were counted and surface area per osteoclast was measured. The data shown are representative of three independent experiments performed in triplicate. **, $p < 0.005$ versus control stable RAW264.7 cells. All data are expressed as mean ± SD.

A

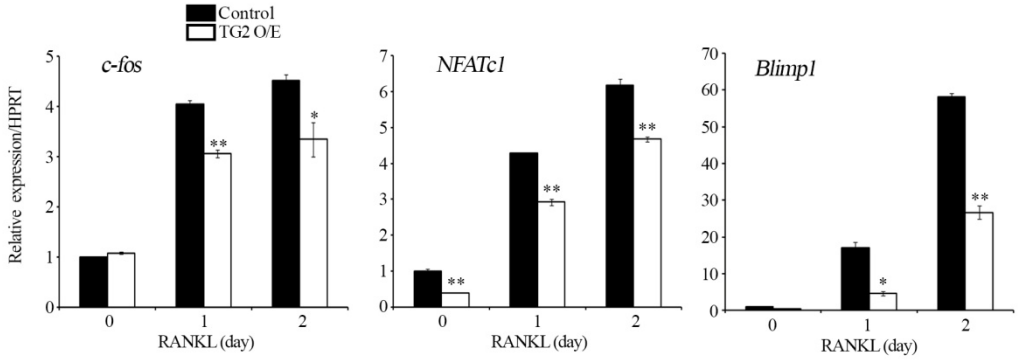

B

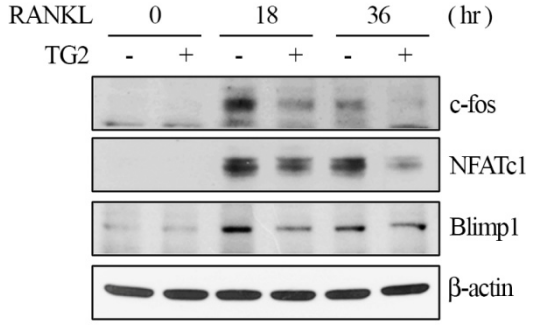

Figure 18. TG2 inhibited osteoclast formation in RAW264.7 cells.

(A) mRNA levels were measured using real-time PCR and were normalized relative to the expression of *HPRT*. (B) Whole cell lysates were subjected to Western blot analysis with indicated antibodies. The data shown are representative of three independent experiments performed in triplicate. *, $p < 0.05$; **, $p < 0.005$ versus control stable RAW264.7 cells. All data are expressed as mean ± SD.

8. TG2 knockout mice exhibits decreased bone mass.

To verify the role of TG2 *in vivo*, bone morphologic parameters in trabecular of the distal femur were analyzed by micro-CT. First, I examined whether TG2 deficiency was able to reduce bone mass in 13wk-old female mice. Three-dimensional micro-CT images of trabecular bone of femurs revealed that the trabecular structure was significantly lower in TG2 knockout mice compared to the wildtype mice (Fig. 19A). Similarly, I analyzed the bone phenotype of TG2 knockout mice using micro-CT. An alteration of the trabecular architecture was found in TG2 knockout mice (Fig. 19B). Accordingly, the micro-CT analysis of distal regions of femur showed significantly lower trabecular bone volume per tissue volume (BV/TV) in TG2 knockout mice (Fig. 19C). Further structural analysis indicated that trabecular thickness (Tb.Th) and trabecular number (Tb.N) were also decreased in TG2 knockout mice (Fig. 19C). Conversely, TG2 deficiency significantly increased the levels of trabecular separation (Tb.sp) (Fig. 19C). To address whether decreased bone mass in TG2 knockout mice was related to increased osteoclastogenesis, I analyzed the histological bone sections that were stained for TRAP and with hematoxylin and eosin (Fig. 20A). Consistent with TG2 knockdown results, TG2 deficiency increased the number

of osteoclasts per bone perimeter (N.Oc/B.Pm) (Fig. 20B). Furthermore, TG2 deficiency also enhanced the levels of osteoclast surface per bone surface (Oc.S/BS) and eroded surface per bone surface (ES/BS). Although TG2 deficiency slightly decreased the number of osteoblasts per bone perimeter (N.Ob/B.Pm), the difference was not statistically significant (Fig. 20B). These observations indicate that TG2 affects the generation of osteoclasts but not osteoblasts in mice.

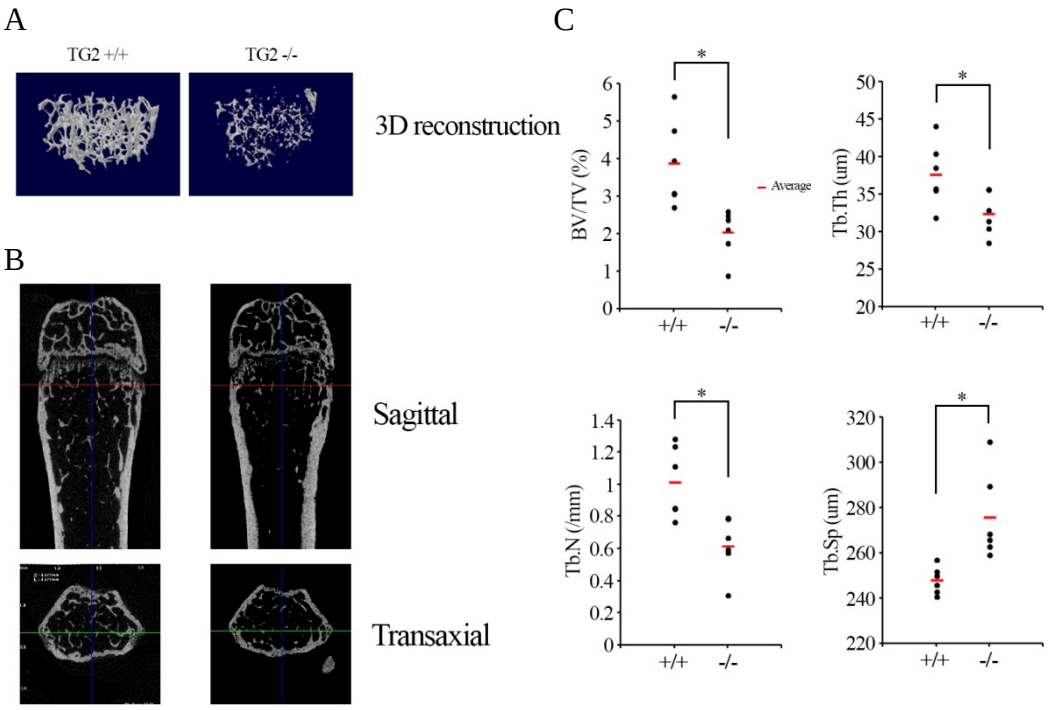

Figure 19. TG2 deficiency decreased trabecular bone and bone parameters.

(A) Three-dimensional micro-CT images of distal femurs of 13-wk old WT and TG2 knockout mice (n = 6 for each group) were reconstructed with Skyscan CTvol software. (B) The sagittal and transaxial images were shown with DataViewer software. (C) The trabecular Bone volume per tissue volume (BV/TV), trabecular thickness (Tb.Th), trabecular number (Tb.N), and trabecular separation (Tb.Sp) in distal femurs were quantified by micro-CT analysis with Skyscan CTAn software. *, $P < 0.05$; **, $p < 0.005$ versus WT mice. All data are expressed as mean ± SD.

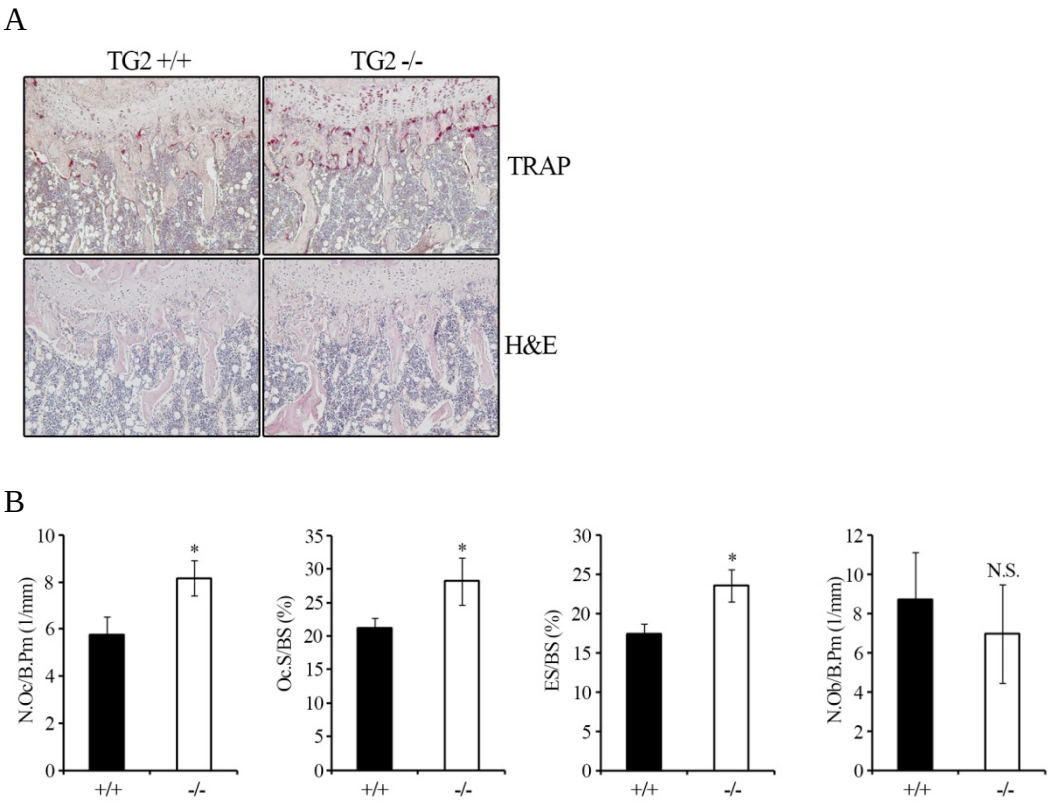

Figure 20. TG2 deficiency increased osteoclast differentiation *in vivo*.

(A) Tissue sections of the distal femur in WT and TG2 knockout mice were stained for TRAP (upper panel). Representative sections of femur, stained with hematoxylin/eosin (H&E), are shown (lower panel). Scale bar, 100 μm. (B) The number of osteoclasts per bone perimeter (N.Oc/B.Pm), osteoclast surface per bone surface (Oc.S/BS), eroded surface per bone surface (ES/BS), and number of osteoblasts per bone perimeter (N.Ob/B.Pm) were quantified (n = 6). *, $P < 0.05$ versus WT mice. NS, no significant difference between groups. All data are expressed as mean ± SD.

9. TG2 knockout increases osteoclast differentiation and expression of c-fos, NFATc1 and Blimp1.

Because histomorphometric analyses indicated that TG2 deficiency increased the number and surface of osteoclasts *in vivo*, I addressed whether TG2 regulates osteoclast differentiation *in vitro* by using TG2 knockout BMMs. To examine this point, BMMs were prepared from WT and TG2 knockout mice. These cells were subjected to *in vitro* osteoclastogenesis by stimulation with RANKL. TG2 deficiency significantly increased number of TRAP-positive MNCs and surface area per osteoclast (Fig. 21A, B). I also found that c-fos, NFATc1 and Blimp1 were significantly increased in TG2 knockout cells (Fig. 22A, B). To address how TG2 regulates osteoclast differentiation, I examined the intracellular localization of NFATc1 in the osteoclast precursors and pOCs. In osteoclast precursors, NFATc1 was localized within the cytoplasmic region before RANKL stimulation. After treatment with RANKL for 2 days, nuclear translocation of NFATc1 was increased in TG2 knockout pOCs (Fig. 23A, B; Lamin B, green; NFATc1, red; TG2, blue; several mononuclear cells are shown). These observations reveal that NFATc1 was translocalized to the nucleus by RANKL stimulation and it was increased by TG2 deficiency. Because of the

observed effect of TG2 deficiency, I further investigated its importance for sealing zone (SZ) formation, given the critical importance of this actin structure in the bone resorption process. The SZ size per osteoclast and the number of actin ring were significant increased the in TG2 knockout osteoclasts compared to control osteoclasts (Fig. 24A, B). These observations indicate that TG2 deficiency increases osteoclastic differentiation and function.

A

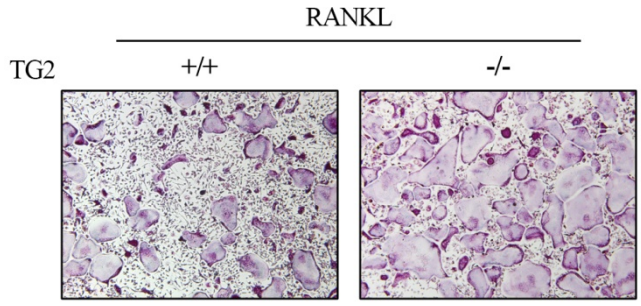

B

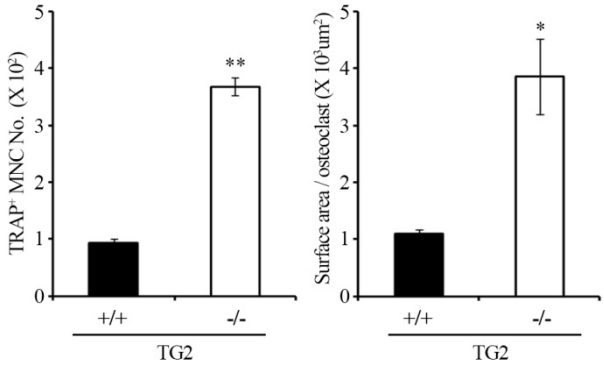

Figure 21. TG2 deficiency enhanced osteoclast formation.

BMMs were obtained from WT and TG2 knockout mice. (A) After treatment with RANKL for 3 days, cells were fixed and stained for TRAP. (B) Number of TRAP-positive MNCs was counted and surface area per osteoclast was measured. The data shown are representative of three independent experiments performed in triplicate. *, $P < 0.05$; **, $p < 0.005$ versus WT BMMs. All data are expressed as mean ± SD.

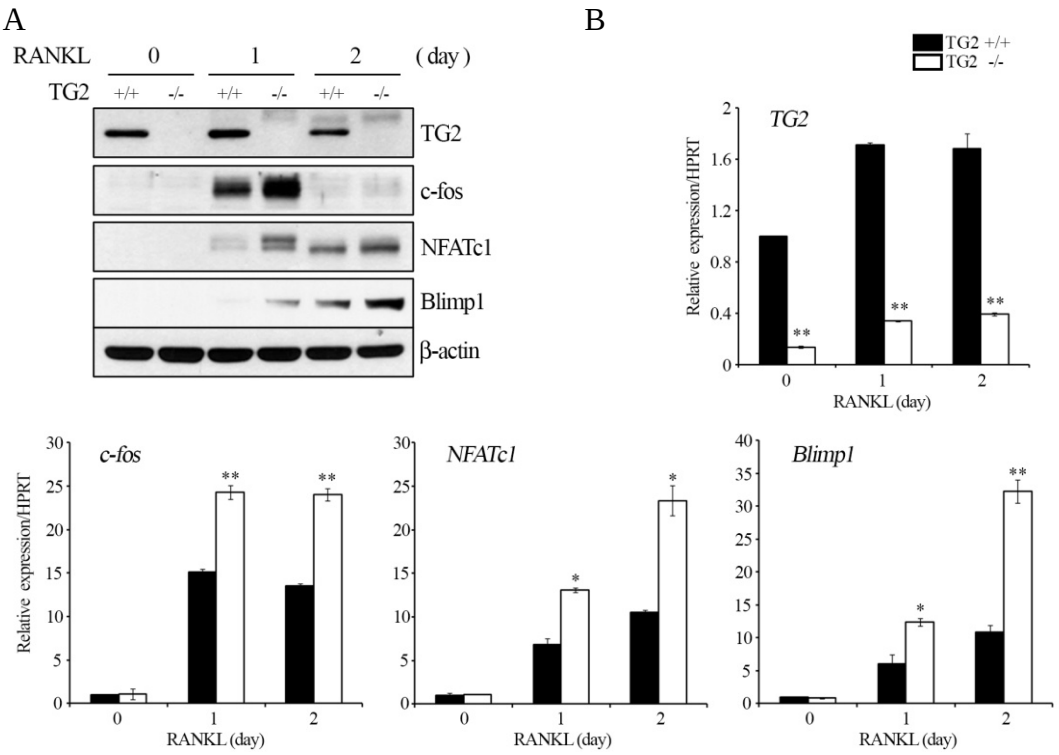

Figure 22. TG2 knockout increased expression of c-fos, NFATc1 and Blimp1.

BMMs were obtained from WT and TG2 knockout mice. (A) Whole cell lysates were analyzed by Western blot analysis using indicated antibodies. (B) mRNA expression levels of *TG2*, *c-fos*, *NFATc1* and *Blimp1* were determined by real-time PCR and normalized with the level of *HPRT*. The data shown are representative of three independent experiments performed in triplicate. *, $P < 0.05$; **, $p < 0.005$ versus WT BMMs. All data are expressed as mean ± SD.

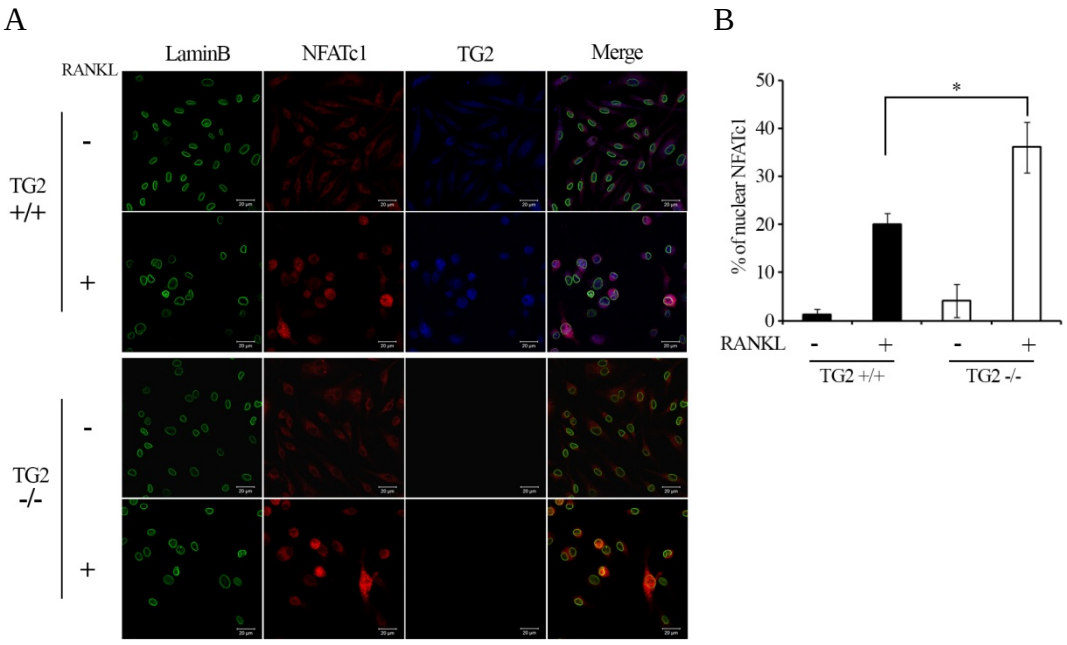

Figure 23. TG2 deficiency induced the nuclear translocation of NFATc1.

BMMs were obtained from WT and TG2 knockout mice. (A) Images of osteoclast precursor cells before treatment with RANKL and cells after treatment with RANKL for 2 days are shown. Cells stained for Lamin B (green), NFATc1 (red) and TG2 (blue) were examined by fluorescence microscopy. Anti-LaminB stained nuclear envelope. (B) Cells with nuclear NFATc1 were counted. The data shown are representative of three independent experiments performed in triplicate. *, $P < 0.05$ versus WT BMMs. All data are expressed as mean ± SD.

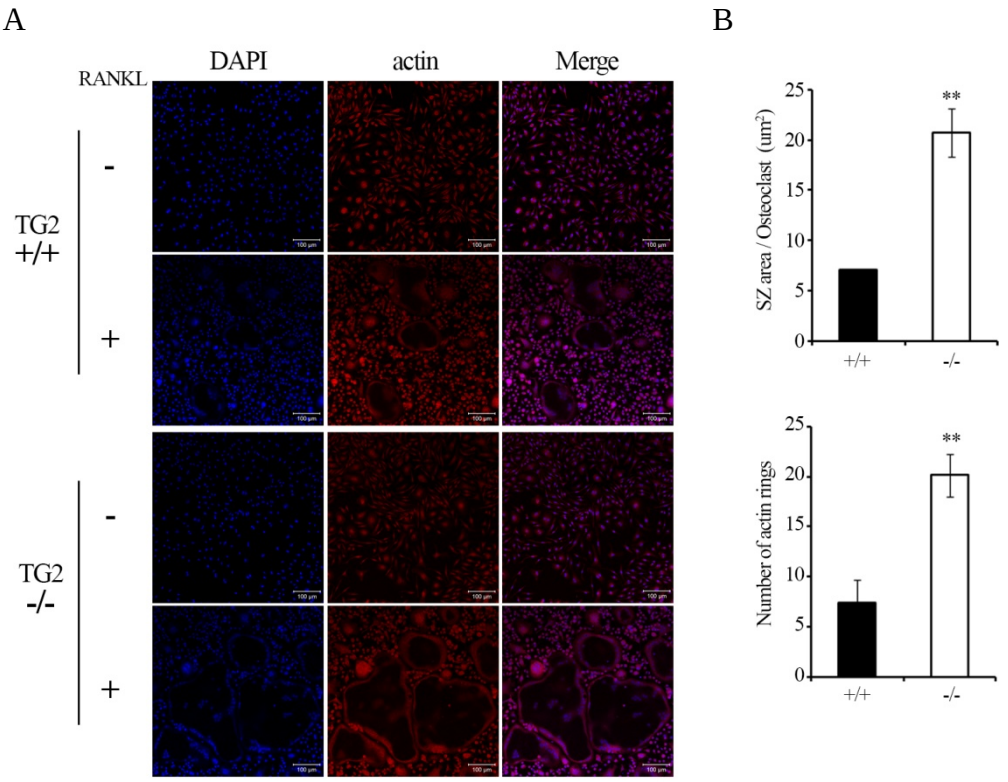

Figure 24. TG2 deficiency enhanced sealing zone formation.

BMMs were obtained from WT and TG2 knockout mice. (A) BMMs were cultured with M-CSF and RANKL for 3 days. Cells were stained with rhodamine-phalloidin (F-actin) and DAPI (nucleus). (B) Sealing zone (SZ) area per osteoclast and number of actin ring were measured. The data shown are representative of three independent experiments performed in triplicate. **, $p < 0.005$ versus WT BMMs. All data are expressed as mean ± SD.

10.TG2 deficiency increases the activation of MAPKs and NF-κB signaling pathways.

To further validate the target signaling pathways affected by TG2 deficiency, I evaluated the activation of MAPKs and NF-κB signaling pathways using the WT and TG2 knockout BMMs. The RANKL-induced phosphorylation of ERK, p38, JNK was augmented in the TG2 knockout BMMs (Fig. 25A). TG2 deficiency had little influence on the total levels of ERK, p38 and JNK. Furthermore, TG2 deficiency did not affect cell proliferation (Fig. 25B). Because TG2 deficiency enhances the activation of ERK, p38 and JNK, I examined effects of MAPK inhibitors on the expression of c-fos and NFATc1 in TG2 knockout BMMs. Treatment of BMMs with MEK inhibitor (U0126) and p38 MAPK inhibitor (SB203580) strongly blocked RANKL-induced c-fos, NFATc1 expression (Fig. 26A, B). In case of JNK signaling, Treatment of BMMs with JNK inhibitor (SP600125) suppressed RANKL-induced phospho-c-Jun and NFATc1 expression, and did not affect c-fos expression level by RANKL (Fig. 26C). These results demonstrate that TG2 regulates osteoclast differentiation through ERK, p38 and JNK signaling pathways. The RANKL-induced IκB phosphorylation was evidently increased at 5 min and the level of

unphosphorylated IκB was further decreased at 30 min by TG2 deficiency (Fig. 27A). When I examined the nuclear translocalization of p65 by RANKL stimulation, TG2 deficiency strongly increased distribution of p65 in the nucleus region of osteoclasts. Quantitative analysis showed that TG2 deficiency increased p65 nuclear translocation in the TG2 knockout BMMs at 15 and 30 min (Fig. 27B). I also confirmed that TG2 deficiency increased p65 nuclear translocation by immunostaining (Fig 28A). RANKL-treated cells showed intense nuclear accumulation of p65 in TG2 knockout BMMs (Fig. 28B). These data indicate that the TG2 deficiency increased the activation of NF-κB signaling pathway by RANKL. Taken together, MAPKs and NF-κB signaling pathways are crucial for TG2-mediated enhancement of osteoclast differentiation.

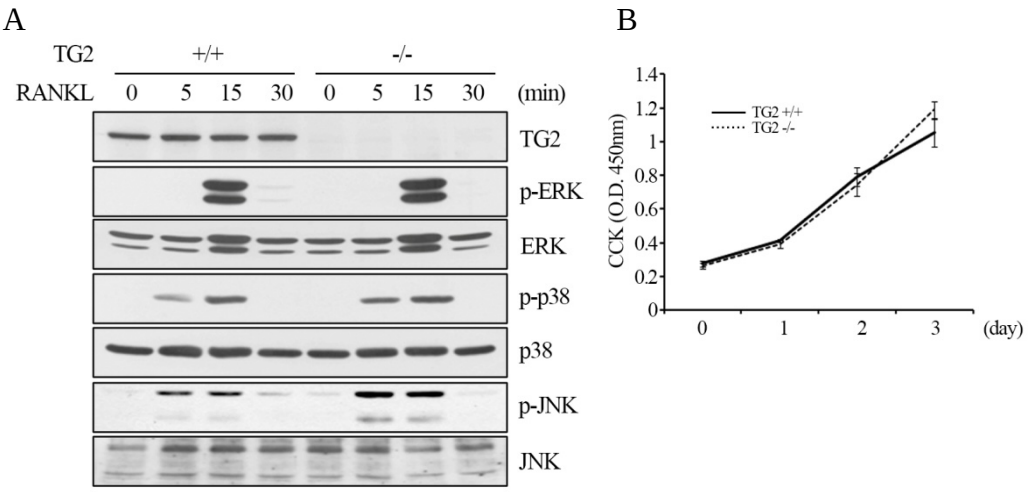

Figure 25. TG2 deficiency increased the activation of MAPKs signaling pathway.

(A) WT and TG2 knockout BMMs were serum-starved for 5 hr and stimulated with RANKL (500 ng/ml) for the indicated times. Whole cell lysates were analyzed by Western blot analysis using MAPKs antibodies. (B) BMMs were cultured at the indicated time and CCK assay was performed. The data shown are representative of three independent experiments performed in triplicate.

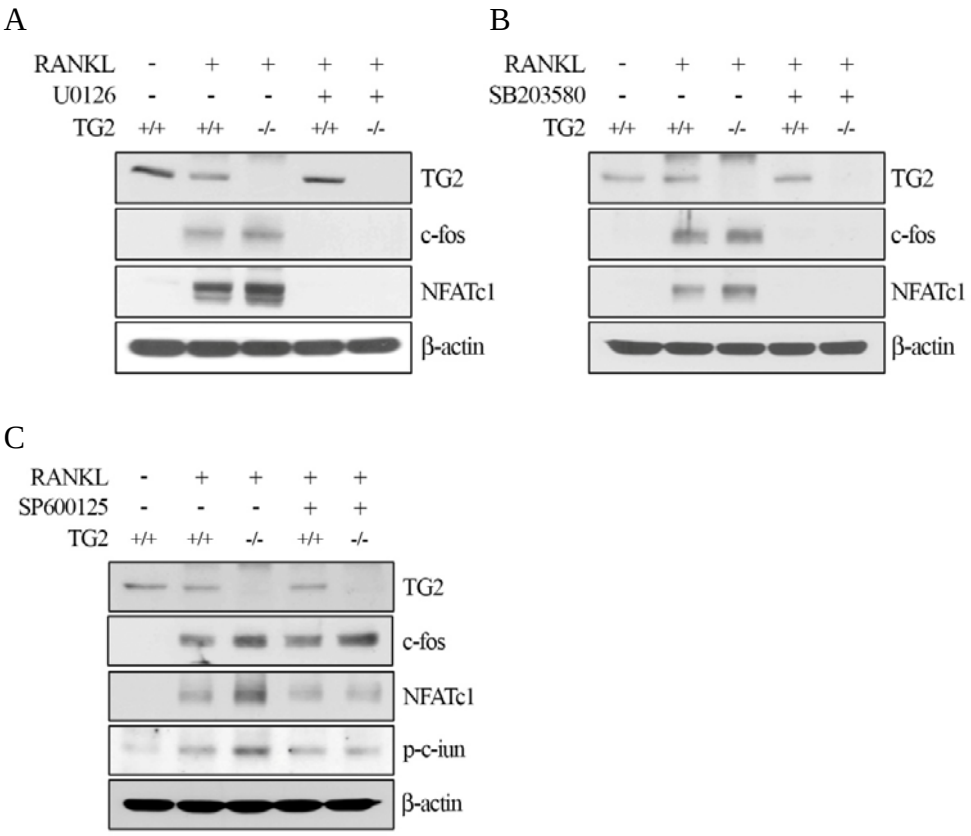

Figure 26. Inhibition of MAPKs attenuated the increase of c-fos, p-c-jun and NFATc1 by TG2 deficiency.

WT and TG2 knockout BMMs were cultured with RANKL for 2 days in the presence of various inhibitors: vehicle (DMSO), U0126 (5 μM), SB203580 (5 μM) or SP600125 (10 μM). Western blot analysis was performed for the expression of indicated proteins. The data shown are representative of three independent experiments.

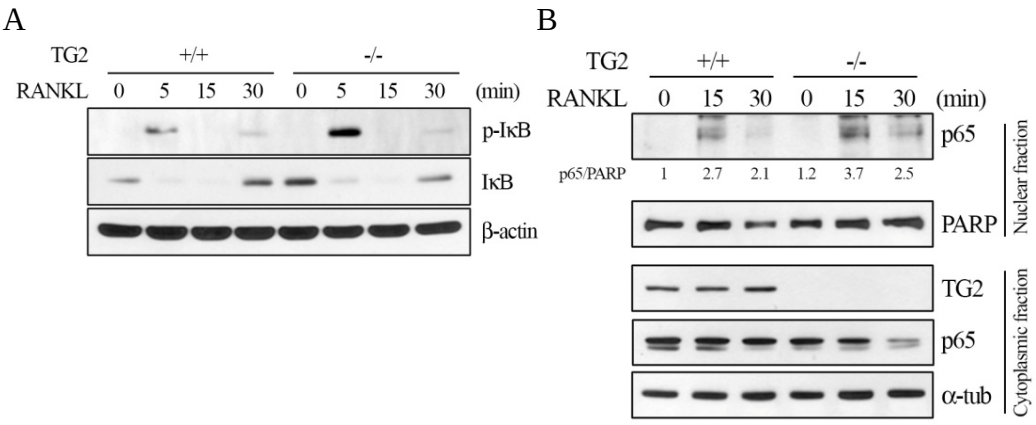

Figure 27. TG2 deficiency enhanced the activation of NF-κB signaling pathway by RANKL.

(A) WT and TG2 knockout BMMs were serum-starved for 5 hr and stimulated with RANKL (500 ng/ml) for the indicated times. Whole cell lysates were analyzed by Western blot analysis using phospho-IκB and IκB antibodies. (B) WT and TG2 knockout BMMs were fractionated and subjected to Western blot analysis with specific antibodies as indicated. Antibodies for α-tubulin and PARP (full length) were used for the normalization of cytoplasmic and nuclear extracts, respectively. Numbers represent densitometrically determined ratios of p65 relative to PARP using ImageJ software (National Institutes of Health, Bethesda, MD). The data shown are representative of three independent experiments.

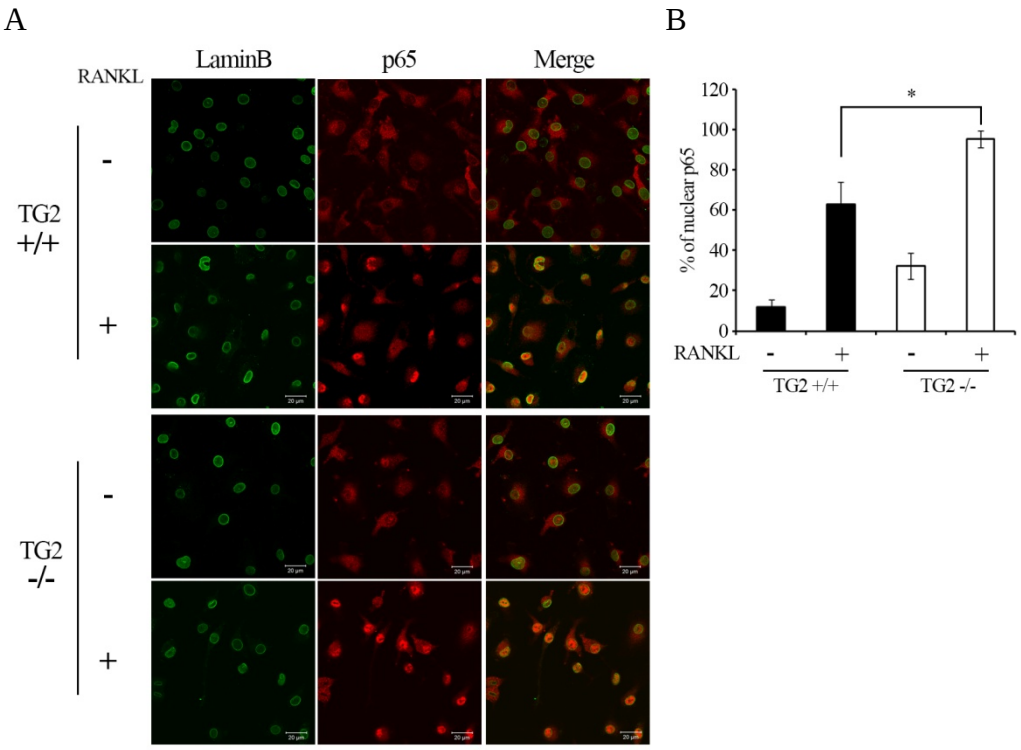

Figure 28. TG2 deficiency increased the nuclear translocation of p65.

BMMs were obtained from WT and TG2 knockout mice. (A) WT and TG2 knockout BMMs were serum-starved for 5 hr and stimulated with or without RANKL (500 ng/ml) for 15 min. Cells stained for Lamin B (green) and p65 (red) were examined by fluorescence microscopy. Anti-LaminB stained nuclear envelope. (B) Cells with nuclear translocated p65 were counted. The data shown are representative of three independent experiments performed in triplicate. *, $P < 0.05$ versus WT BMMs. All data are expressed as mean ± SD.

IV. Discussion

Osteoclasts are derived from the hematopoietic lineage cell and activated to become mature bone-resorbing cells through the expression of transcription factors and functional proteins. Previous studies have demonstrated that transglutaminase activity is critical for regulating the cell adhesion, matrix secretion, deposition and differentiation of osteoblasts, and that inhibition of TG activity blocked these functions. However, TG2 has not yet been examined in osteoclast differentiation. In this study, I observed that TG2 was involved in osteoclastogenesis *in vitro* and *in vivo*. The important role of TG2 was revealed using the loss- and gain-of function approaches. First of all, I found that TG2 was selectively expressed in BMMs and pOCs compared to other TG family members. TG2 knockdown significantly increased the RANKL-induced osteoclast formation. It could elevate the expression of RANKL-induced c-fos and NFATc1. I also observed that expression of osteoclast fusion and resorption related genes, such as *TRAP*, *DC-STAMP* and *Atp6v0d2* was enhanced by TG2 deficiency. Consequently, TG2 silencing resulted in an enhancement of bone resorption activity. TG2 could enhance the activation of NF-κB and MAPKs signaling pathways which have been reported to be involved in osteoclast

differentiation and action by RANKL. Furthermore, the inhibitory effect of TG2 on osteoclast differentiation was confirmed by TG2-overexpressing stable RAW264.7 cells. TG2 overexpression down-regulated the osteoclast formation and expression level of c-fos and NFATc1. These results provide the evidence for that TG2 acts as a negative regulator of osteoclast differentiation and activity.

The underlying molecular signaling mechanism responsible for TG2 mediated suppression of osteoclastogenesis was explored. One candidate is Blimp1, which is a master regulator in hematopoietic lineage cell development, maturation of B lymphocyte, and dendritic cell homeostatic development and function (Chan et al., 2009; Sciammas and Davis, 2004; Turner et al., 1994). Previous studies showed that Blimp1 expression was increased in B cells and T cells from TG2 knockout mice, indicating a potential relationship between Blimp1 and TG2 (Kim et al., 2012). Blimp1 expression was increased by activation of NF-κB signaling pathway (Sen, 2006; Wang et al., 2009). Although Blimp1 enhances NFATc1 expression by suppression of negative regulators in osteoclast differentiation (Zhao and Ivashkiv, 2011), it is largely unclear how Blimp1 regulates osteoclast differentiation. My data confirmed results of the previous studies that RANKL treatment significantly induced the expression of Blimp1 mRNA and protein, and TG2 deficiency more elevated

Blimp1 expression in BMMs and pOCs. NF-κB inhibitor, BAY 11-7085, treatment inhibited expression of Blimp1. Down-regulation of Blimp1 by siRNA or NF-κB inhibitor attenuated the increase of mRNA and protein levels of NFATc1 by TG2 knockdown. I also found that Blimp1 knockdown inhibited the increase of osteoclast formation by TG2 knockdown. Moreover, RANKL-induced nuclear translocation of NFATc1 and Blimp1 was more increased by TG2 knockdown. As a result, I suggest that transcriptional activity of NFATc1 was increased in TG2 knockdown cells. These data indicated that activation of NF-κB signaling pathway by TG2 knockdown increased Blimp1 expression. And Blimp1 directly enhanced expression and transcriptional activity of NFATc1.

The *in vivo* significance of TG2 was investigated by comparing bone phenotypes between TG2 knockout and wildtype mice. TG2 knockout mice showed lower bone mass than wildtype mice. TG2 deficiency increased osteoclast number and surface area, as well as eroded surface in femur sections. In contrast to osteoclasts, TG2 deficiency did not significantly affect osteoblast number *in vivo*. Therefore, increased bone loss in TG2 knockout mice was due to the increase of osteoclast number and bone resorption but was not dependent on regulation of osteoblast number or bone formation. Similarly, *in vitro* experiments showed that BMMs obtained from TG2 knockout mice had

increased formation of TRAP-positive MNCs and expression of c-fos, NFATc1 and Blimp1. Importantly, the nuclear translocation of NFATc1 and p65 was increased in TG2 knockout BMMs by RANKL stimulation.

The MAPKs (ERK, JNK and p38) have been reported to be activated by RANKL stimulation, resulting in the activation of activating protein 1 (AP-1) complex. AP-1 complex containing c-fos and c-jun is required for the induction of NFATc1. The c-fos and c-jun were induced by ERK and p38 (Ang et al., 2011; Huang et al., 2006; Wagner and Matsuo, 2003), and JNK (Ikeda et al., 2004) signaling pathways for osteoclastogenesis, respectively. In this study, I evaluated the effects of TG2 on the activation of three MAPKs and found that TG2 deficiency promoted the phosphorylation of MAPKs. Moreover, treatment of each MAPK inhibitor attenuated the increase of c-fos, phospho-c-Jun and NFATc1 in TG2 knockout BMMs. These results demonstrate that TG2 deficiency contributes to the osteoclastogenic effect partly through promoting phosphorylation of MAPKs in RANKL-stimulated BMMs. Figure 29 depicts a proposed mechanism by which TG2 regulates osteoclast differentiation. Briefly, TG2 down-regulation increases activation of NF-κB and MAPKs signaling pathways which lead to the induction of Blimp1, and c-fos and c-jun, respectively. Sequentially, expression and nuclear translocation of NFATc1, Which is a master transcription factor for osteoclastogenesis, are increased. As

a result, osteoclastogenesis and osteoclast activity are enhanced.

In conclusion, this study provides evidence for inhibitory effects of TG2 on osteoclast differentiation and function, and suggests that TG2 is a potential therapeutic target for the treatment of bone destructive diseases such as osteoporosis and rheumatoid arthritis.

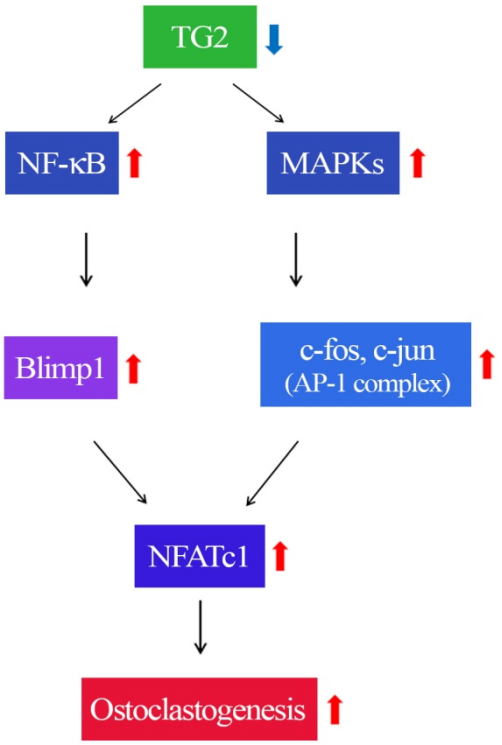

Figure 29. Schematic illustration of a proposed mechanism by which TG2 regulates osteoclastogenesis.

Reduction of TG2 enhances the activation of NF-κB and MAPKs signaling pathways, which increase the expression levels of Blimp1, and c-fos and c-jun, respectively. Blimp1 together with c-fos and c-jun augments expression and nuclear translocation of NFATc1. Finally, osteoclastogenesis and osteoclast activity are stimulated.

V. References

Akimov, S.S., and A.M. Belkin. 2001. Cell surface tissue transglutaminase is involved in adhesion and migration of monocytic cells on fibronectin. *Blood*. 98:1567-1576.

Al-Jallad, H.F., V.D. Myneni, S.A. Piercy-Kotb, N. Chabot, A. Mulani, J.W. Keillor, and M.T. Kaartinen. 2011. Plasma membrane factor XIIIA transglutaminase activity regulates osteoblast matrix secretion and deposition by affecting microtubule dynamics. *PloS one*. 6:e15893.

Al-Jallad, H.F., Y. Nakano, J.L. Chen, E. McMillan, C. Lefebvre, and M.T. Kaartinen. 2006. Transglutaminase activity regulates osteoblast differentiation and matrix mineralization in MC3T3-E1 osteoblast cultures. *Matrix biology*. 25:135-148.

Ang, E., Q. Liu, M. Qi, H.G. Liu, X. Yang, H. Chen, M.H. Zheng, and J. Xu. 2011. Mangiferin attenuates osteoclastogenesis, bone resorption, and RANKL-induced activation of NF-kappaB and ERK. *Journal of cellular biochemistry*. 112:89-97.

Arai, F., T. Miyamoto, O. Ohneda, T. Inada, T. Sudo, K. Brasel, T. Miyata, D.M. Anderson, and T. Suda. 1999. Commitment and differentiation of osteoclast precursor cells by the sequential expression of c-Fms and receptor activator of nuclear factor kappaB (RANK) receptors. *The Journal of experimental medicine*. 190:1741-1754.

Asagiri, M., K. Sato, T. Usami, S. Ochi, H. Nishina, H. Yoshida, I. Morita, E.F. Wagner, T.W. Mak, E. Serfling, and H. Takayanagi. 2005. Autoamplification of NFATc1 expression determines its essential role in

bone homeostasis. *The Journal of experimental medicine*. 202:1261-1269.

Asagiri, M., and H. Takayanagi. 2007. The molecular understanding of osteoclast differentiation. *Bone*. 40:251-264.

Balajthy, Z., K. Csomos, G. Vamosi, A. Szanto, M. Lanotte, and L. Fesus. 2006. Tissue-transglutaminase contributes to neutrophil granulocyte differentiation and functions. *Blood*. 108:2045-2054.

Barone, M.V., I. Caputo, M.T. Ribecco, M. Maglio, R. Marzari, D. Sblattero, R. Troncone, S. Auricchio, and C. Esposito. 2007. Humoral immune response to tissue transglutaminase is related to epithelial cell proliferation in celiac disease. *Gastroenterology*. 132:1245-1253.

Begg, G.E., L. Carrington, P.H. Stokes, J.M. Matthews, M.A. Wouters, A. Husain, L. Lorand, S.E. Iismaa, and R.M. Graham. 2006a. Mechanism of allosteric regulation of transglutaminase 2 by GTP. *Proceedings of the National Academy of Sciences of the United States of America*. 103:19683-19688.

Begg, G.E., S.R. Holman, P.H. Stokes, J.M. Matthews, R.M. Graham, and S.E. Iismaa. 2006b. Mutation of a critical arginine in the GTP-binding site of transglutaminase 2 disinhibits intracellular cross-linking activity. *The Journal of biological chemistry*. 281:12603-12609.

Boyle, W.J., W.S. Simonet, and D.L. Lacey. 2003. Osteoclast differentiation and activation. *Nature*. 423:337-342.

Braun, T., and J. Zwerina. 2011. Positive regulators of osteoclastogenesis and bone resorption in rheumatoid arthritis. *Arthritis research & therapy*. 13:235.

Calame, K.L., K.I. Lin, and C. Tunyaplin. 2003. Regulatory mechanisms that

determine the development and function of plasma cells. *Annual review of immunology*. 21:205-230.

Chan, Y.H., M.F. Chiang, Y.C. Tsai, S.T. Su, M.H. Chen, M.S. Hou, and K.I. Lin. 2009. Absence of the transcriptional repressor Blimp-1 in hematopoietic lineages reveals its role in dendritic cell homeostatic development and function. *Journal of immunology*. 183:7039-7046.

Dardik, R., T. Krapp, E. Rosenthal, J. Loscalzo, and A. Inbal. 2007. Effect of FXIII on monocyte and fibroblast function. *Cellular physiology and biochemistry*. 19:113-120.

Datta, S., M.A. Antonyak, and R.A. Cerione. 2007. GTP-binding-defective forms of tissue transglutaminase trigger cell death. *Biochemistry*. 46:14819-14829.

De Laurenzi, V., and G. Melino. 2001. Gene disruption of tissue transglutaminase. *Molecular and cellular biology*. 21:148-155.

Di Venere, A., A. Rossi, F. De Matteis, N. Rosato, A.F. Agro, and G. Mei. 2000. Opposite effects of Ca(2+) and GTP binding on tissue transglutaminase tertiary structure. *The Journal of biological chemistry*. 275:3915-3921.

Fesus, L., and Z. Szondy. 2005. Transglutaminase 2 in the balance of cell death and survival. *FEBS letters*. 579:3297-3302.

Georgess, D., M. Mazzorana, J. Terrado, C. Delprat, C. Chamot, R.M. Guasch, I. Perez-Roger, P. Jurdic, and I. Machuca-Gayet. 2014. Comparative transcriptomics reveals RhoE as a novel regulator of actin dynamics in bone-resorbing osteoclasts. *Molecular biology of the cell*. 25:380-396.

Griffin, M., R. Casadio, and C.M. Bergamini. 2002. Transglutaminases: nature's biological glues. *The Biochemical journal*. 368:377-396.

Grigoriadis, A.E., Z.Q. Wang, M.G. Cecchini, W. Hofstetter, R. Felix, H.A.

Fleisch, and E.F. Wagner. 1994. c-Fos: a key regulator of osteoclast-macrophage lineage determination and bone remodeling. *Science*. 266:443-448.

Gupta, S., A. Anthony, and A.B. Pernis. 2001. Stage-specific modulation of IFN-regulatory factor 4 function by Kruppel-type zinc finger proteins. *Journal of immunology*. 166:6104-6111.

Harada, S., and G.A. Rodan. 2003. Control of osteoblast function and regulation of bone mass. *Nature*. 423:349-355.

Hayashi, S., T. Yamane, A. Miyamoto, H. Hemmi, H. Tagaya, Y. Tanio, H. Kanda, H. Yamazaki, and T. Kunisada. 1998. Commitment and differentiation of stem cells to the osteoclast lineage. *Biochemistry and cell biology = Biochimie et biologie cellulaire*. 76:911-922.

Heath, D.J., S. Downes, E. Verderio, and M. Griffin. 2001. Characterization of tissue transglutaminase in human osteoblast-like cells. *Journal of bone and mineral research*. 16:1477-1485.

Huang, H., E.J. Chang, J. Ryu, Z.H. Lee, Y. Lee, and H.H. Kim. 2006. Induction of c-Fos and NFATc1 during RANKL-stimulated osteoclast differentiation is mediated by the p38 signaling pathway. *Biochemical and biophysical research communications*. 351:99-105.

Iismaa, S.E., B.M. Mearns, L. Lorand, and R.M. Graham. 2009. Transglutaminases and disease: lessons from genetically engineered mouse models and inherited disorders. *Physiological reviews*. 89:991-1023.

Iismaa, S.E., M.J. Wu, N. Nanda, W.B. Church, and R.M. Graham. 2000. GTP binding and signaling by Gh/transglutaminase II involves distinct residues in a unique GTP-binding pocket. *The Journal of biological*

chemistry. 275:18259-18265.

Ikeda, F., R. Nishimura, T. Matsubara, S. Tanaka, J. Inoue, S.V. Reddy, K. Hata, K. Yamashita, T. Hiraga, T. Watanabe, T. Kukita, K. Yoshioka, A. Rao, and T. Yoneda. 2004. Critical roles of c-Jun signaling in regulation of NFAT family and RANKL-regulated osteoclast differentiation. *The Journal of clinical investigation*. 114:475-484.

Inada, R., M. Matsuki, K. Yamada, Y. Morishima, S.C. Shen, N. Kuramoto, H. Yasuno, K. Takahashi, Y. Miyachi, and K. Yamanishi. 2000. Facilitated wound healing by activation of the Transglutaminase 1 gene. *The American journal of pathology*. 157:1875-1882.

Iotsova, V., J. Caamano, J. Loy, Y. Yang, A. Lewin, and R. Bravo. 1997. Osteopetrosis in mice lacking NF-kappaB1 and NF-kappaB2. *Nature medicine*. 3:1285-1289.

Johnson, K., M. Shapiro-Shelef, C. Tunyaplin, and K. Calame. 2005. Regulatory events in early and late B-cell differentiation. *Molecular immunology*. 42:749-761.

Kanehisa, J., T. Yamanaka, S. Doi, K. Turksen, J.N. Heersche, J.E. Aubin, and H. Takeuchi. 1990. A band of F-actin containing podosomes is involved in bone resorption by osteoclasts. *Bone*. 11:287-293.

Kang, S.K., K.S. Yi, N.S. Kwon, K.H. Park, U.H. Kim, K.J. Baek, and M.J. Im. 2004. Alpha1B-adrenoceptor signaling and cell motility: GTPase function of Gh/transglutaminase 2 inhibits cell migration through interaction with cytoplasmic tail of integrin alpha subunits. *The Journal of biological chemistry*. 279:36593-36600.

Keller, A.D., and T. Maniatis. 1991. Identification and characterization of a novel repressor of beta-interferon gene expression. *Genes &*

development. 5:868-879.

Khosla, S. 2001. Minireview: the OPG/RANKL/RANK system. *Endocrinology*. 142:5050-5055.

Kim, J.H., E.M. Jeong, Y.J. Jeong, W.J. Lee, J.S. Kang, I.G. Kim, and Y.I. Hwang. 2012. Transglutaminase 2 modulates antigen-specific antibody response by suppressing Blimp-1 and AID expression of B cells in mice. *Immunology letters*. 147:18-28.

Kim, K., J.H. Kim, J. Lee, H.M. Jin, H. Kook, K.K. Kim, S.Y. Lee, and N. Kim. 2007. MafB negatively regulates RANKL-mediated osteoclast differentiation. *Blood*. 109:3253-3259.

Kim, K., S.H. Lee, J. Ha Kim, Y. Choi, and N. Kim. 2008. NFATc1 induces osteoclast fusion via up-regulation of Atp6v0d2 and the dendritic cell-specific transmembrane protein (DC-STAMP). *Molecular endocrinology*. 22:176-185.

Kim, S.Y., T.M. Jeitner, and P.M. Steinert. 2002. Transglutaminases in disease. *Neurochemistry international*. 40:85-103.

Kukita, T., N. Wada, A. Kukita, T. Kakimoto, F. Sandra, K. Toh, K. Nagata, T. Iijima, M. Horiuchi, H. Matsusaki, K. Hieshima, O. Yoshie, and H. Nomiyama. 2004. RANKL-induced DC-STAMP is essential for osteoclastogenesis. *The Journal of experimental medicine*. 200:941-946.

Kwon, H., D. Thierry-Mieg, J. Thierry-Mieg, H.P. Kim, J. Oh, C. Tunyaplin, S. Carotta, C.E. Donovan, M.L. Goldman, P. Tailor, K. Ozato, D.E. Levy, S.L. Nutt, K. Calame, and W.J. Leonard. 2009. Analysis of interleukin-21-induced Prdm1 gene regulation reveals functional cooperation of STAT3 and IRF4 transcription factors. *Immunity*. 31:941-952.

Lee, S.H., J. Rho, D. Jeong, J.Y. Sul, T. Kim, N. Kim, J.S. Kang, T. Miyamoto,

T. Suda, S.K. Lee, R.J. Pignolo, B. Koczon-Jaremko, J. Lorenzo, and Y. Choi. 2006. v-ATPase V0 subunit d2-deficient mice exhibit impaired osteoclast fusion and increased bone formation. *Nature medicine*. 12:1403-1409.

Lorand, L., and R.M. Graham. 2003. Transglutaminases: crosslinking enzymes with pleiotropic functions. *Nature reviews. Molecular cell biology*. 4:140-156.

Martin, T.J., and N.A. Sims. 2005. Osteoclast-derived activity in the coupling of bone formation to resorption. *Trends in molecular medicine*. 11:76-81.

Martins, G., and K. Calame. 2008. Regulation and functions of Blimp-1 in T and B lymphocytes. *Annual review of immunology*. 26:133-169.

Martins, G.A., L. Cimmino, M. Shapiro-Shelef, M. Szabolcs, A. Herron, E. Magnusdottir, and K. Calame. 2006. Transcriptional repressor Blimp-1 regulates T cell homeostasis and function. *Nature immunology*. 7:457-465.

Morgan, M.A., E. Magnusdottir, T.C. Kuo, C. Tunyaplin, J. Harper, S.J. Arnold, K. Calame, E.J. Robertson, and E.K. Bikoff. 2009. Blimp-1/Prdm1 alternative promoter usage during mouse development and plasma cell differentiation. *Molecular and cellular biology*. 29:5813-5827.

Mukherjee, A., and P. Rotwein. 2012. Selective signaling by Akt1 controls osteoblast differentiation and osteoblast-mediated osteoclast development. *Molecular and cellular biology*. 32:490-500.

Nahrendorf, M., K. Hu, S. Frantz, F.A. Jaffer, C.H. Tung, K.H. Hiller, S. Voll, P. Nordbeck, D. Sosnovik, S. Gattenlohner, M. Novikov, G. Dickneite, G.L. Reed, P. Jakob, A. Rosenzweig, W.R. Bauer, R. Weissleder, and G. Ertl. 2006. Factor XIII deficiency causes cardiac rupture, impairs wound

healing, and aggravates cardiac remodeling in mice with myocardial infarction. *Circulation*. 113:1196-1202.

Nakashima, T., and H. Takayanagi. 2011. New regulation mechanisms of osteoclast differentiation. *Annals of the New York Academy of Sciences*. 1240:E13-18.

Nishikawa, K., T. Nakashima, M. Hayashi, T. Fukunaga, S. Kato, T. Kodama, S. Takahashi, K. Calame, and H. Takayanagi. 2010. Blimp1-mediated repression of negative regulators is required for osteoclast differentiation. *Proceedings of the National Academy of Sciences of the United States of America*. 107:3117-3122.

Nurminskaya, M., and M.T. Kaartinen. 2006. Transglutaminases in mineralized tissues. *Frontiers in bioscience*. 11:1591-1606.

Nurminskaya, M., C. Magee, L. Faverman, and T.F. Linsenmayer. 2003. Chondrocyte-derived transglutaminase promotes maturation of preosteoblasts in periosteal bone. *Developmental biology*. 263:139-152.

Ohinata, Y., B. Payer, D. O'Carroll, K. Ancelin, Y. Ono, M. Sano, S.C. Barton, T. Obukhanych, M. Nussenzweig, A. Tarakhovsky, M. Saitou, and M.A. Surani. 2005. Blimp1 is a critical determinant of the germ cell lineage in mice. *Nature*. 436:207-213.

Quan, G., J.Y. Choi, D.S. Lee, and S.C. Lee. 2005. TGF-beta1 up-regulates transglutaminase two and fibronectin in dermal fibroblasts: a possible mechanism for the stabilization of tissue inflammation. *Archives of dermatological research*. 297:84-90.

Reddy, S.V., J.E. Hundley, J.J. Windle, O. Alcantara, R. Linn, R.J. Leach, D.H. Boldt, and G.D. Roodman. 1995. Characterization of the mouse tartrate-resistant acid phosphatase (TRAP) gene promoter. *Journal of bone and*

mineral research. 10:601-606.

Reljic, R., S.D. Wagner, L.J. Peakman, and D.T. Fearon. 2000. Suppression of signal transducer and activator of transcription 3-dependent B lymphocyte terminal differentiation by BCL-6. *The Journal of experimental medicine*. 192:1841-1848.

Saltel, F., O. Destaing, F. Bard, D. Eichert, and P. Jurdic. 2004. Apatite-mediated actin dynamics in resorbing osteoclasts. *Molecular biology of the cell*. 15:5231-5241.

Sarang, Z., P. Molnar, T. Nemeth, S. Gomba, T. Kardon, G. Melino, S. Cotecchia, L. Fesus, and Z. Szondy. 2005. Tissue transglutaminase (TG2) acting as G protein protects hepatocytes against Fas-mediated cell death in mice. *Hepatology*. 42:578-587.

Sciammas, R., and M.M. Davis. 2004. Modular nature of Blimp-1 in the regulation of gene expression during B cell maturation. *Journal of immunology*. 172:5427-5440.

Sciammas, R., A.L. Shaffer, J.H. Schatz, H. Zhao, L.M. Staudt, and H. Singh. 2006. Graded expression of interferon regulatory factor-4 coordinates isotype switching with plasma cell differentiation. *Immunity*. 25:225-236.

Sen, R. 2006. Control of B lymphocyte apoptosis by the transcription factor NF-kappaB. *Immunity*. 25:871-883.

Shapiro-Shelef, M., K.I. Lin, L.J. McHeyzer-Williams, J. Liao, M.G. McHeyzer-Williams, and K. Calame. 2003. Blimp-1 is required for the formation of immunoglobulin secreting plasma cells and pre-plasma memory B cells. *Immunity*. 19:607-620.

Smink, J.J., V. Begay, T. Schoenmaker, E. Sterneck, T.J. de Vries, and A. Leutz.

2009. Transcription factor C/EBPbeta isoform ratio regulates osteoclastogenesis through MafB. *The EMBO journal*. 28:1769-1781.

Steinert, P.M., E. Candi, E. Tarcsa, L.N. Marekov, M. Sette, M. Paci, B. Ciani, P. Guerrieri, and G. Melino. 1999. Transglutaminase crosslinking and structural studies of the human small proline rich 3 protein. *Cell death and differentiation*. 6:916-930.

Steinert, P.M., S.Y. Kim, S.I. Chung, and L.N. Marekov. 1996. The transglutaminase 1 enzyme is variably acylated by myristate and palmitate during differentiation in epidermal keratinocytes. *The Journal of biological chemistry*. 271:26242-26250.

Sturniolo, M.T., S.R. Dashti, A. Deucher, E.A. Rorke, A.M. Broome, R.A. Chandraratna, T. Keepers, and R.L. Eckert. 2003. A novel tumor suppressor protein promotes keratinocyte terminal differentiation via activation of type I transglutaminase. *The Journal of biological chemistry*. 278:48066-48073.

Suda, T., N. Takahashi, N. Udagawa, E. Jimi, M.T. Gillespie, and T.J. Martin. 1999. Modulation of osteoclast differentiation and function by the new members of the tumor necrosis factor receptor and ligand families. *Endocrine reviews*. 20:345-357.

Takayanagi, H., S. Kim, T. Koga, H. Nishina, M. Isshiki, H. Yoshida, A. Saiura, M. Isobe, T. Yokochi, J. Inoue, E.F. Wagner, T.W. Mak, T. Kodama, and T. Taniguchi. 2002. Induction and activation of the transcription factor NFATc1 (NFAT2) integrate RANKL signaling in terminal differentiation of osteoclasts. *Developmental cell*. 3:889-901.

Tehrani, S., R. Faccio, I. Chandrasekar, F.P. Ross, and J.A. Cooper. 2006. Cortactin has an essential and specific role in osteoclast actin assembly.

Molecular biology of the cell. 17:2882-2895.

Teitelbaum, S.L. 2000. Bone resorption by osteoclasts. *Science*. 289:1504-1508.

Teitelbaum, S.L., M.M. Tondravi, and F.P. Ross. 1997. Osteoclasts, macrophages, and the molecular mechanisms of bone resorption. *Journal of leukocyte biology*. 61:381-388.

Turner, C.A., Jr., D.H. Mack, and M.M. Davis. 1994. Blimp-1, a novel zinc finger-containing protein that can drive the maturation of B lymphocytes into immunoglobulin-secreting cells. *Cell*. 77:297-306.

Valledor, A.F., F.E. Borras, M. Cullell-Young, and A. Celada. 1998. Transcription factors that regulate monocyte/macrophage differentiation. *Journal of leukocyte biology*. 63:405-417.

Vasanwala, F.H., S. Kusam, L.M. Toney, and A.L. Dent. 2002. Repression of AP-1 function: a mechanism for the regulation of Blimp-1 expression and B lymphocyte differentiation by the B cell lymphoma-6 protooncogene. *Journal of immunology*. 169:1922-1929.

Vincent, S.D., N.R. Dunn, R. Sciammas, M. Shapiro-Shalef, M.M. Davis, K. Calame, E.K. Bikoff, and E.J. Robertson. 2005. The zinc finger transcriptional repressor Blimp1/Prdm1 is dispensable for early axis formation but is required for specification of primordial germ cells in the mouse. *Development*. 132:1315-1325.

Wagner, E.F., and R. Eferl. 2005. Fos/AP-1 proteins in bone and the immune system. *Immunological reviews*. 208:126-140.

Wagner, E.F., and K. Matsuo. 2003. Signalling in osteoclasts and the role of Fos/AP1 proteins. *Annals of the rheumatic diseases*. 62 Suppl 2:ii83-85.

Wagner, H. 2010. Bone diseases: Interferon regulatory factor-8 suppresses osteoclastogenesis. *Nature reviews. Rheumatology*. 6:73-74.

Walsh, M.C., N. Kim, Y. Kadono, J. Rho, S.Y. Lee, J. Lorenzo, and Y. Choi. 2006. Osteoimmunology: interplay between the immune system and bone metabolism. *Annual review of immunology*. 24:33-63.

Wang, X., K. Belguise, C.F. O'Neill, N. Sanchez-Morgan, M. Romagnoli, S.F. Eddy, N.D. Mineva, Z. Yu, C. Min, V. Trinkaus-Randall, D. Chalbos, and G.E. Sonenshein. 2009. RelB NF-kappaB represses estrogen receptor alpha expression via induction of the zinc finger protein Blimp1. *Molecular and cellular biology*. 29:3832-3844.

Wong, B.R., R. Josien, S.Y. Lee, M. Vologodskaia, R.M. Steinman, and Y. Choi. 1998. The TRAF family of signal transducers mediates NF-kappaB activation by the TRANCE receptor. *The Journal of biological chemistry*. 273:28355-28359.

Yagi, M., T. Miyamoto, Y. Sawatani, K. Iwamoto, N. Hosogane, N. Fujita, K. Morita, K. Ninomiya, T. Suzuki, K. Miyamoto, Y. Oike, M. Takeya, Y. Toyama, and T. Suda. 2005. DC-STAMP is essential for cell-cell fusion in osteoclasts and foreign body giant cells. *The Journal of experimental medicine*. 202:345-351.

Yu, Z., S. Sato, P.C. Trackman, K.H. Kirsch, and G.E. Sonenshein. 2012. Blimp1 activation by AP-1 in human lung cancer cells promotes a migratory phenotype and is inhibited by the lysyl oxidase propeptide. *PloS one*. 7:e33287.

Yuan, L., K. Choi, C. Khosla, X. Zheng, R. Higashikubo, M.R. Chicoine, and K.M. Rich. 2005. Tissue transglutaminase 2 inhibition promotes cell death and chemosensitivity in glioblastomas. *Molecular cancer therapeutics*. 4:1293-1302.

Zemskov, E.A., A. Janiak, J. Hang, A. Waghray, and A.M. Belkin. 2006. The

role of tissue transglutaminase in cell-matrix interactions. *Frontiers in bioscience*. 11:1057-1076.

Zhao, B., and L.B. Ivashkiv. 2011. Negative regulation of osteoclastogenesis and bone resorption by cytokines and transcriptional repressors. *Arthritis research & therapy*. 13:234.

Zhao, B., M. Takami, A. Yamada, X. Wang, T. Koga, X. Hu, T. Tamura, K. Ozato, Y. Choi, L.B. Ivashkiv, H. Takayanagi, and R. Kamijo. 2009. Interferon regulatory factor-8 regulates bone metabolism by suppressing osteoclastogenesis. *Nature medicine*. 15:1066-1071.

ABSTRACT IN KOREAN

RANKL에 의해 유도되는 파골세포 분화과정에서 Transglutaminase 2의 역할

서울대학교 대학원 세포및발생생물학 전공

(지도교수 : 김 홍 희)

김 우 신

Transglutaminase 2 (TG2)은 transglutaminase, protein kinase, cell surface adhesion mediator, G protein, protein disulfide isomerase, isopeptidase 와 같은 다양한 기능을 가진 단백질이다. 골 대사 연구분야에서 fibronectin 과 type I collagen matrix deposition에 중요하다고 알려져 있지만 TG2 기능 중 파골세포 형성 (osteoclastogenesis)에 관한 연구는 아직 명확히 이루어지지 않은 상태이다. 따라서 본 연구를 통해 TG2가 파골세포 형성을 조절하는지 여부를 밝히고자 하였다. 우선 TG family 중 TG2가 파골 전구세포와 파골세포에서 가장 많이 발현되는 것을 발견하였다. 또한 TG2 siRNA와 TG2 knockout 마우스를 이용하여 파골세포 분화에서 TG2의 역할이 무엇인지 연구하였다. TG2 발현이 억제되었을 때 파골세포 분화에 중요한 전사인자인 c-fos와 NFATc1의 발현이 증가되는 것을 확인하였고 파골세포에 중요한 MAPKs와 NF-κB 신호전달을 확인한 결과 TG2가 결핍되어있을 때 더 증가되는 것을 확인하였다. 또한 파골세포 분화에 중요한 전사인자 중 NFATc1과 p65가 TG2의 발현이 억제되었을

때 핵으로 더 많이 이동된 것을 관찰할 수 있었다. 반대로 TG2의 발현이 증가되었을 때는 c-fos와 NFATc1의 발현과 파골세포 형성이 억제되는 것을 확인하였다. Blimp1은 파골세포 분화를 증가시키는 기능을 가지고 있고 NF-κB 신호전달을 통해 발현이 증가된다는 것으로 보고되어 있다. 또한 TG2는 Blimp1의 발현을 억제한다고 알려져 있어 파골세포 분화에서 TG2와 Blimp1의 연관성을 연구하였다. TG2의 발현이 억제되었을 때 Blimp1의 발현이 증가되는 것을 확인하였고 TG2 발현억제로 인한 c-fos와 NFATc1의 발현과 파골세포 증가현상은 Blimp1의 발현 억제를 통해 그 현상이 감소 되는 것을 확인하였다.

이러한 현상들이 마우스의 뼈에서도 관찰 되는지 알아보기 위해 TG2 결핍 마우스의 뼈를 이용하여 뼈 지표인자를 분석한 결과 TG2가 결핍된 마우스에서 뼈의 양이 감소된 것을 확인하였고 뼈 조직염색법을 이용하여 파골세포의 수와 면적은 증가되어있는 것을 관찰하였다.

따라서 이러한 결과를 통해 TG2가 Blimp1을 통해 파골세포 분화와 기능을 억제하는 역할을 한다는 것을 알 수 있었다.

주요어 : 파골세포 분화, Transglutaminase 2, c-fos, NFATc1, NF-κB, Blimp1

학 번 : 2009-31131